

Mapping Urban Floods in 2023: A Study Using Sentinel-1 SAR and Social Media Data Validation.

M.Tech. Thesis

By

Anjali Patel



M.Tech

INDIAN INSTITUTE OF TECHNOLOGY INDORE

MAY 2024

Mapping Urban Floods in 2023: A Study Using Sentinel-1 SAR and Social Media Data Validation.

A THESIS

Submitted in partial fulfillment of the requirements for the award of the degree of
Master of Technology

By
Anjali Patel



**DEPARTMENT OF ASTRONOMY, ASTROPHYSICS, AND
SPACE ENGINEERING**

INDIAN INSTITUTE OF TECHNOLOGY INDORE

MAY 2024



INDIAN INSTITUTE OF TECHNOLOGY INDORE

CANDIDATE'S DECLARATION

I hereby certify that the work which is being presented in the thesis entitled **Mapping Urban Floods in 2023: A Study Using Sentinel-1 SAR and Social Media Data Validation** in the partial fulfillment of the requirements for the award of the degree of **M.Tech** and submitted in the **Department Of Astronomy, Astrophysics And Space Engineering, Indian Institute of Technology Indore**, is an authentic record of my own work carried out during the time period from **JULY 2023** to **MAY 2024** under the supervision of **Dr. Unmesh Khati**.

The matter presented in this thesis has not been submitted by me for the award of any other degree of this or any other institute.

**Signature of the student with date
(NAME OF THE CANDIDATE)**

This is to certify that the above statement made by the candidate is correct to the best of my knowledge.

26/4/2024

Signature of the Supervisor of
M.Tech. thesis
DR. UNMESH KHATI

Anjali Patel has successfully given his/her M.Tech. Oral Examination held on **26 April 2024**.

Signature(s) of Supervisor(s) of M.Tech thesis
Date: 26/04/2024

Programme Coordinator, M.Tech.
Date: 24/05/2024

Convenor, DPGC
Date: 24/05/2024

Head, DAASE
Date:

ACKNOWLEDGEMENTS

I want to express my sincere appreciation to Dr. Unmesh Khati, my thesis advisor, for her steadfast support and guidance throughout the entirety of this research endeavor. Dr. Khati's insightful comments and constructive criticism played a pivotal role in refining and shaping my ideas. Their unwavering dedication to this project has proven to be invaluable.

My gratitude extends to the faculty and staff at DAASE, with a special acknowledgement to the members of the Remote Sensing Lab. Their encouragement and support during my tenure as a graduate student have been instrumental. The wealth of expertise and knowledge within the lab has significantly enriched my academic journey, offering valuable insights into remote sensing.

Additionally, I wish to recognize the contributions of my colleagues and classmates. Their unwavering friendship, support, and encouragement have been constants throughout my studies. The camaraderie and collaborative spirit they fostered were a continuous source of inspiration and motivation.

To everyone who has played a role in my academic journey, thank you for your unwavering support and encouragement.

.

Abstract

This study focuses on mapping urban floods in 2023 in the cities of Delhi, Chennai, Nagpur, and Greece, using Sentinel-1 Synthetic Aperture Radar (SAR) imagery and social media data for validation. The research applies rule-based classification, change detection, and supervised classification methods to identify flooded areas. By plotting histograms for pre-flood and post-flood images, a threshold of -30 dB is chosen to determine flooded pixels. Permanent water is distinguished using the Global Surface Water (GSW) dataset, with pixels having a seasonality band greater than 5 considered as permanent water. Noise reduction is accomplished through isolated pixel masking, eliminating single pixels in areas with fewer than eight connected neighbors.

Historical and current flood maps from the Indian Space Research Organization (ISRO) provide the foundation for training data in supervised classification. Validation of the methods is achieved using crowd-sourced data from social media platforms such as Twitter and Facebook, as well as news channels and OpenCity. The study concludes by plotting confusion matrices for each method against ground truth data, assessing the accuracy of the proposed flood mapping approaches.

Keywords: urban floods, SAR imagery, rule-based classifier, change detection, supervised classification, social media validation, confusion matrix.

TABLE OF CONTENTS

LIST OF FIGURES

LIST OF TABLES

NOMENCLATURE

ACRONYMS (if any)

INDIAN INSTITUTE OF TECHNOLOGY INDORE	i
CANDIDATE'S DECLARATION.....	i
ACKNOWLEDGEMENTS	ii
Chapter 1 Introduction	1
1.1 Natural Hazard	1
1.2 Natural disaster.....	2
1.3 Flood.....	3
1.4 Motivation and Problem Statement.....	5
1.5 Research questions	6
1.6 Structure of the thesis.....	7
Chapter 2 Literature Review	9
2.1 Remote Sensing and Flood Inundation Mapping	9
2.2 Microwave Remote Sensing for Flood Inundation Mapping.....	11
2.3 Conventional Techniques	11
2.4 Advanced Techniques	13
Chapter 3 Study Area	15
3.1 Location.....	15

3.2 Physiography and Geomorphology	16
3.3 Drainage Network and Sub-basin.....	17
3.4 Climate	18
3.5 Soil and vegetation	20
3.6 Economic Aspect.....	21
3.7 Demography	24
3.8 Road Networks.....	24
3.9 Canal Network.....	25
Chapter 4 Material and Methods.....	27
4.1 Introduction to SENTINEL.....	27
4.2 SENTINEL Data Products	30
4.3 Pre-Processing of Sentinel data.....	30
4.4 Overall Methodology and Software used.....	32
4.5 Extraction of flooded areas	33
4.6 Mask used in algorithm	39
4.7 Change Detection Technique	42
4.8 Random Forest	42
4.9 Methodology for Extracting Geotagged Social Media Flooded Pictures	44
Chapter 5 Results	49
5.1 Delhi Results	50
5.2 Chennai Results.....	54
5.3 Nagpur Results	58

5.4 Greece Results.....	61
Chapter 6 Conclusion.....	65
6.1 Future Work	65

List of figures:

Fig 1: Location of study.....	15
Fig 2: Acquisition modes	29
Fig 3: Sentinel-1 Ground Range Detected (GRD) preprocessing workflow.....	32
Fig 4: Flowchart for methodology	33
Fig 5: Histogram Before/After (Delhi, Chennai, Nagpur, Greece).....	35
Fig 6: Reference Flood Map/Sample training data.....	36
Fig 7: In-situ Floods images 2023-credits: Forbes	39
Fig 8: Chennai Flood 2023-Twitter	43
Fig 9: Crowd-sourced data – Social media	44
Fig 10: Filtered images of Delhi, before and after the flood	50
Fig 11: a) Rule based classification, and b) Change Detection	51
Fig 12: a) Rule-based classification, and b) Change detection	51
Fig 13: Random Forest	52
Fig 14: Reference Flood map from NRSC for Delhi.....	53
Fig 15: Before Flood.....	54
Fig 16: After Flood.....	54
Fig 17: Rule based classification	54
Fig 18: Change detection	55

Fig 19: Random Forest	56
Fig 20: Comparison amongst methods for Chennai	57
Fig 21: Before Flood	58
Fig 22: After Flood	58
Fig 23: Rule based classification	59
Fig 24: Change detection	59
Fig 25: Random Forest	60
Fig 26: Comparison amongst methods for Nagpur	60
Fig 27: Before Flood	61
Fig 28: After Flood	61
Fig 29: Rule based classification	61
Fig 30: Change detection	62
Fig 31: Random Forest	63
Fig 32: Comparison amongst methods for Nagpur	64

List of tables:

Table 1: Sentinel Specifications	28
Table 2: Sentinel antenna specifications	29
Table 3: Representation of key elements related to the Algorithm and Data used	34

Chapter 1

Introduction

1.1 Natural Hazard

Before humans exerted influence on Earth, the planet operated under a natural system where geophysical events like earthquakes, volcanic eruptions, landslides, and river plain dynamics unfolded over millions of years. This pristine state of nature drastically transformed with human presence, labeling the once-natural phenomena as 'natural hazards.' Human interference has not only altered the natural system but has also given a new perspective and term to the geophysical events of the past.

The term 'natural hazard' refers to occurrences of natural conditions or phenomena posing a threat or hazard within a specific space and time. Originally, these hazards were elements in the physical environment that had the potential to harm humans. Over time, with increased human influence, what were once natural hazards in the pre-modern era have evolved into 'man-induced natural disasters'.

Natural disasters, encompassing various extreme weather-related events such as floods and cyclones, have surged in frequency and intensity globally in recent years. This shift is a consequence of increased human influence on the environment (Khan and Rahman, 2007).

Natural hazards can cause immediate and long-term damage to both the physical and social environment where they occur. They are broadly categorized into geological events (earthquakes, volcanoes, landslides) and hydro-meteorological events (floods, storms, droughts, tsunamis). Hazards arise from sudden changes in long-term behavior, influenced by minute alterations in initial conditions. Geomorphic hazards fall into categories.

Events like hurricanes, earthquakes, storms, and disease outbreaks

highlight an increasing trend in economic and human losses. Lack of specific knowledge about these hazardous events is identified as a significant factor contributing to such losses (Ermolieva and Sergienko, 2008). Assessing natural hazards involves understanding concepts like magnitude, frequency, and time. For instance, the consequences of a flood are evaluated using the concept of return period, indicating the flood's likely magnitude and frequency. Natural hazards occur in specific locations and during defined periods, and their development is not instantaneous.

Time plays a crucial role in the occurrence and progression of these phenomena. For instance, flooding triggered by tropical storms takes time to develop as specific atmospheric conditions lead to storm formation over hours to days. Therefore, the intensity and duration of rainfall over time are vital factors in determining flooding characteristics.

1.2 Natural disaster

Various definitions of natural disasters offer a nuanced understanding of the term. In the 1960s, disasters were perceived as uncontrollable events posing severe danger, and disrupting essential societal functions. The concept portrayed a society damaged by a potent natural force, where a disaster is characterized as severe, sudden, and lethal—such as flooding resulting from a breach in embankment, as witnessed along the Indo-Nepal border in 2008. The interaction between an unstable earth and an unresting human element can lead to general disruption, loss of life, and property destruction for vulnerable human groups.

In the present context, a disaster is recognized as a significant disruption to society's functioning, causing widespread human, material, or environmental loss beyond the affected society's capacity to cope using its own resources. This understanding considers not only the natural aspect but also the impact on social and economic systems. A natural disaster is framed as a rapid, instantaneous impact of the natural environment on the socio-economic system or a sudden imbalance between the forces released by the natural system and the

counteracting forces of society. The severity of this imbalance hinges on the relationship between the magnitude of the natural event and human tolerance.

While the number of lives lost has decreased in the past two decades, the total number of people affected has surged. Over the last decade, the total number of people impacted by natural disasters has tripled to 2 billion. Noy (2008) emphasizes that countries with higher literacy rates, robust institutions, greater per capita income, openness to trade, and higher government spending can better withstand the initial shock of a disaster. Developing countries, grappling with poverty and population pressure, face heightened vulnerability as people settle in flood-prone or landslide-susceptible areas.

Lack of widespread education and awareness, coupled with poor economic, social, political, and cultural conditions, contributes to the vulnerability of these areas and their populations to natural disasters. Recent attention has been directed toward the prevention, reduction, and mitigation of natural disasters, marked by the creation of the Scientific and Technical Committee of the International Decade for Natural Disaster Reduction (IDNDR). Efforts within this international framework are global, acknowledging that changes at the micro-level can accumulate and impact the world on a larger scale (e.g., global warming), while global phenomena can influence local levels. The interdependence of nations, institutions, and technologies continues to grow as efforts intensify to comprehend not only natural phenomena but also the role of anthropogenic activities in causing and modifying them. Although preventing natural phenomena is beyond human capability, scientists gain a better understanding of the factors behind disasters, providing valuable knowledge to disaster management agencies, enhancing preparedness for extreme events (Zadeh and Bear, 2007).

1.3 Flood

River valleys and floodplains have served as the cradle of civilizations since ancient times and remain some of the most densely populated regions

globally. The high population density near rivers makes floods the most prevalent natural disaster, affecting more people worldwide than all other natural or technological disasters combined and inflicting significant human hardship and economic losses (Huang et al., 2008). Flooding typically results from heavy or continuous rainfall surpassing the soil's absorptive capacity and the flow capacity of river channels and streams. The natural variability in river flow makes flooding a recurring event. In many parts of the world where populations are concentrated along river valleys, floods pose a greater threat than any other natural hazard.

While floodplains are valuable resources in agricultural economies, human activities on these floodplains have elevated the potential for floods to cause damage and disrupt lives, a risk likely to increase with further encroachment (Sultana et al., 2008).

Defining when high flows become floods depends on perspective. Physically, floods involve high water flow that overtops natural or artificial embankments. Ecologically, floods constitute overbank flows providing water and nutrients to floodplains. Geomorphologically, high flows become floods when they alter the erosive, transport, and depositional capacity of a river, changing the morphology of the river channel and surrounding floodplain. From a human perspective, a river is in floods when its waters invade human settlements and agriculture, resulting in fatalities and damage to livelihoods (Ologunorisa and Adeyemo, 2005).

Flood events can result from various natural and human-induced factors, causing known damages to life, property, and economic activity disruption. Given that floodplains are hubs of human activities, the potential for damage is exacerbated. Minimizing flood damage necessitates comprehensive measures related to prediction, prevention, warning, monitoring, and relief along a floodplain. Undertaking these measures requires an in-depth analysis of factors causing (natural) and modifying (anthropogenic) floodwater spread. Effective flood management requires interaction between different government and private

agencies and the affected population to utilize scientific knowledge for damage reduction. However, flood management interventions may have complex and sometimes unforeseen impacts on both the natural and human environment, making studies and research on floods challenging and intriguing.

India stands as one of the most severely flood-affected countries globally, ranking second only to Bangladesh in terms of flood-related damages. Approximately 75% of India's annual rainfall occurs during the four-month monsoon period (June-September), leading to substantial water discharge in rivers. The flood

risk is exacerbated by issues such as sediment deposition, drainage congestion, and the synchronization of river floods with sea tides in coastal plains. The increased use of fossil fuels, extensive deforestation, and the rapid expansion of rice cultivation using nitrogen-based chemical fertilizers in India, Nepal, and Bangladesh contribute to greenhouse warming, resulting in a heightened frequency of flood events in the region (Ali, 2007).

The flood-vulnerable area encompasses around 0.4 million km², with an average annual flood-affected area of about 0.08 million km². The cropped area affected annually ranges from 3.5 million hectares during normal floods to 10 million hectares during severe floods. Flood control measures primarily involve the construction of new embankments, drainage channels, and afforestation aimed at preventing the loss of life and property caused by floods.

1.4 Motivation and Problem Statement

In the past few decades, as existing urban centers have expanded and there has been a proliferation of new second and third tier cities in India, the phenomenon of urban floods has become increasingly common (Anjaria,2006;Gupta and Nair,2011;Ramachandraiah,2011). Flooding in an urbanized catchment with a dense built environment, higher population density and greater density of economic assets and infrastructure, equates to

exponentially more loss per unit area as compared to rural landscapes. As a result, studying the production and impacts of urban inundation has been crucial to planners and city governments. For a large part of the post-independence era the government of India has treated floods as riverine or coastal phenomena and addressed them at the scale of a river basin (Mohapatra and Singh,2003). The National Disaster Management Authority of India in its first disaster management manual of 2008 classified floods as a natural hydrological disaster or event. Although the manual focused largely on basin scale management it did recognize urban flooding as a special category of disaster for which separate guidelines would be prepared in the future. The subject of urban flooding has been recognized by the NDMA as one meriting exclusive attention and separate guidelines for its management because of the fact that the 2008 manual was preceded by some extreme urban flood event such as the Mumbai floods of 2005 that saw an exponentially larger loss of life, assets and urban infrastructure per unit area than before. In 2010 the NDMA came out with a separate manual for urban flooding that tackled the various aspects of its production, management, response, recovery and mitigation. This classification carried through even in the most recent NDMA Manual 2016 that states : “The problem of urban flooding is a result of both natural factors and land-use changes brought about by urban development. Urban flooding is significantly different from rural flooding as urbanization leads to developed catchments which increases the flood peaks from 1.8 to 8 times and flood volumes by up to 6 times. Consequently, flooding occurs very quickly due to faster flow times, sometimes in a matter of minutes.”(NDMA Guidelines Management of Urban Flooding, 2016). Thus it is safe to establish that urban floods need to be understood from a unique lens that takes into account the ecological and urban processes to assess the extent of damage and suggest strategies for mitigation.

1.5 Research questions

1. What method is better suited for identifying inundated areas in SENTINEL data?

2. What are the most effective methods for validating flood mapping results using social media data in these urban areas?
3. What improvements can be made in flood mapping by integrating historical flood maps, ground truth data, and crowd-sourced data?
4. What supplementary data contributes to enhancing the precision of the extraction process and facilitating the interpretation of outcomes?

1.6 Structure of the thesis

The present research is organized into six chapters, each focusing on specific aspects of the study. Chapter one serves as an introduction, presenting the concepts of natural hazards, natural disasters, and the specific focus on floods. It highlights the significance of studying floods in the delta region of Nagpur, Chennai, Delhi, and Greece, emphasizing the need for the research. The main objectives and specific research questions are outlined.

Chapter two provides an overview of the geographical aspects (physical, human, and economic) of the study area. Understanding these aspects is crucial for result analysis and for justifying the research from academic, social, and economic perspectives.

In the third chapter, a literature review is conducted to establish the originality of the proposed work, contextualize it, and compare different methodological approaches.

Chapter four details the characteristics of the datasets used in the study. It also provides a comprehensive description of the methodology applied, presenting results obtained through visual and digital techniques for extracting flood- inundated areas.

The analysis is covered in chapter five, where the results of various techniques are compared, and the accuracy of these techniques is assessed based on ancillary information and field observations.

The concluding chapter, chapter six, summarizes major findings and offers suggestions and recommendations for accurately and efficiently mapping and

monitoring flood extents using remote sensing and GIS. It concludes by proposing further studies to address not only flood-related challenges but also to enhance the overall understanding of floods in Delhi.

The research is designed to address the complexities posed by geomorphic variability and human habitation in mapping flood events using a remote sensing approach. Local-scale flood flow paths, influenced by anthropogenic activities, are explored, necessitating high-resolution satellite data for accurate recording. Field verification becomes crucial to fill gaps in understanding factors controlling the extent of floodwater spread over time.

While flood extent can be mapped using various visual and digital techniques, accuracy depends on ancillary information and a profound understanding of the inundated surface. Validation of results from different techniques can be achieved by applying the same methods to an image of a flood event in the same area but from a different date, preferably a different year, to better comprehend similarities and differences in results.

Chapter 2

Literature Review

2.1 Remote Sensing and Flood Inundation Mapping

Accurate information regarding the extent of water bodies is crucial for effective flood prediction, monitoring, and relief efforts (Smith, 1997). Traditional ground-based survey methods can be challenging during floods due to inaccessibility and safety concerns. The synoptic and repetitive capabilities of satellite-based remote sensing have become a powerful tool for near real-time flood inundation mapping, aiding in relief, damage assessment, and flood management. Remote sensing techniques offer promise in determining flood extent, duration, depth, and associated hazards.

Satellite remote sensing provides valuable insights into flood magnitude by correlating the extent of flooding with the severity of the flood. It also enables the extraction of flood duration and inundation patterns using multiple satellite data over the same area. Beyond immediate flood response, remote sensing contributes to flood plain land use mapping, supports flood forecasting and warning systems, maps river channel migration, and identifies chronic flood-prone areas. In the long term, remote sensing proves to be a cost-effective and efficient technique for comprehensive studies covering large areas.

In the early stages of satellite remote sensing, Landsat Multi-Spectral Scanner (MSS) data with 80m resolution, specifically MSS band 7 (0.8–1.1 μm), were utilized for delineating water or moist soil due to the strong absorption of water in the near-infrared spectrum (Smith, 1997). Landsat Thematic Mapper (TM) images with 30m resolution since the 1980s became a major data source for monitoring floods and delineating inundation boundaries. SPOT multi-spectral imageries were also employed in flood delineation, leveraging the low reflectance of water in the near-infrared spectrum, particularly in regions like Bangladesh (Oberstadler et al., 1997; Sado and Islam, 1997).

Coarse-resolution imagery, such as Advanced Very High-Resolution Radiometer (AVHRR) data, proves valuable for floods with extensive coverage (Islam and Sado, 2000). In cases of large flood-affected areas, the use of very high-resolution data may not be practical due to the need for numerous scenes to cover the entire area. NOAA (National Oceanographic Atmospheric Administrative) data, particularly NOAA- AVHRR, is advantageous in such studies due to its high frequency of global coverage, wide swath, high repeatability, and cost-effectiveness, enabling near real-time flood monitoring (Jain et al., 2006).

To enhance water detection using the near-infrared band, the Normalized Difference Vegetation Index (NDVI) is employed to monitor rivers in AVHRR images. Water exhibits a distinctive spectral signature in the near-infrared region, differing significantly from other surface features. Wang et al. (2002) note that NDVI values for inundated surfaces remain negative, while non-inundated surfaces typically have values greater than 0. However, the choice of threshold is critical, considering variations in natural river flooding conditions across different locations. Factors like atmospheric conditions, cloud cover, and satellite viewing angles also impact NDVI values and should be considered before calculation (Sanyal and Lu, 2003).

Over the past decade, Indian Remote Sensing (IRS) satellites, including the IRS series with sensors like LISS-I, LISS-II, and PAN, have provided flood information for various regions in the country. The IRS satellites offer optical information at spatial resolutions ranging from 72m to 5.8m and repetitive coverage intervals from 5 to 24 days. WiFS sensor data from IRS satellites plays a crucial role in flood monitoring due to its broad swath, high repeatability, and frequent coverage during critical flood periods. Additionally, NRSA receives data from meteorological satellites such as NOAA (AVHRR). While optical remote sensing faces challenges in mapping and monitoring flooded terrain due to dense vegetation and cloud cover, microwave data provides a solution by penetrating clouds (Rashid and Pramanik, 1993; Melack et al., 1994).

2.2 Microwave Remote Sensing for Flood Inundation Mapping

Radar imagery, specifically Synthetic Aperture Radar (SAR), possesses the capability to penetrate the atmosphere under various weather conditions. Microwave energy used in SAR can penetrate through elements like haze, light rain, snow, clouds, and smoke. Unlike optical sensors, microwave reflections or emissions in SAR do not correlate directly with visible or thermal spectra, offering independent environmental information about landscape features. SAR operates actively, eliminating dependence on natural illumination, and its microwave frequencies can penetrate cloud cover, providing a unique all-weather, day/night capability, particularly advantageous in flood management applications (Matgen et al., 2007).

In comparison to optical sensors like SPOT and LANDSAT, SAR imagery from sensors such as SENTINEL, RADARSAT, ERS, and JERS captures energy transmitted at microwave frequencies, undetectable by the human eye. RADARSAT, operating at a single microwave frequency, produces black and white images. As an active sensor, SAR transmits microwave energy pulses directly towards the Earth's surface, measuring the energy that returns after interacting with the surface. Unlike optical sensors, RADARSAT's microwave energy can penetrate through clouds, rain, dust, or haze, allowing data collection under various atmospheric conditions. SAR, and SENTINEL in particular, are effective in detecting open surface water, making them valuable for flood monitoring applications worldwide (Brisco et al., 2008).

2.3 Conventional Techniques

Satellite data analysis for flood mapping typically employs visual interpretation or digital image processing techniques. Visual interpretation relies on the fact that water surfaces, being smoother than dry land, exhibit low backscatter, providing reasonably accurate assessments of water spread. However, this manual method is time-consuming, prompting the use of digital

techniques for faster flood extent mapping, crucial in relief and rescue operations.

Digital analysis involves various automatic information extraction algorithms. **Thresholding**, a common technique, sets a radar backscatter threshold value in decibels to classify pixels as 'flooded' or 'non-flooded.' The choice of an appropriate threshold often involves trial and error or, in this case study, benefits from control points measured at the inundation boundary. Contrast depends on polarization, SAR system incidence angle, and ground conditions.

Change detection is a powerful tool for flood area detection in SAR imagery, utilizing coherence and amplitude approaches. Amplitude change detection identifies flooded areas where radar backscatter significantly declines post-flood. Coherence change detection identifies flooded areas with low coherence or correlation between radar backscatters before and after a flood. Multi-date SAR scenes can be combined to create a color composite for enhanced visualization.

SAR data, particularly at L-band, has proven effective in mapping inundation in forested wetlands. Studies in various regions, including the Brazilian Amazon and the Rhine valley, showcase SAR's ability to discriminate flood stages. L-band radar, in particular, provides superior flooding distinction in forested areas compared to C-band radar. SAR data has been extensively used in modeling flood inundation, combining GIS with radar and optical remote sensing.

Overall, SAR imagery, with its all-weather capability and penetration through various atmospheric conditions, offers significant advantages, especially in flood management applications. It has been successfully applied in diverse geographic settings, demonstrating its effectiveness in mapping and monitoring flooded areas.

2.4 Advanced Techniques

The nature of the Earth's surface, particularly the vegetation, significantly influences the delineation of water using Synthetic Aperture Radar (SAR) images. In areas with rice cultivation, bogs, and marshes, distinguishing water from short vegetation can be challenging due to the impact of protruding vegetation on backscatter values. Researchers have explored the use of polarimetric radar and the integration of radar with optical remote sensing data for discriminating short emergent vegetation and mapping forested wetlands.

Object-oriented image segmentation and active contour models have been employed for flood extent mapping, leveraging both spectral and spatial information.

Studies emphasize the importance of multiple reflections between water surfaces and upright vegetation, enhancing backscattering in flooded vegetation. Mathematical models have been developed to understand these interactions and assess the influence of radar look angle, wavelength, and polarization on backscatter. Additionally, phase information in SAR imagery has been explored for flood mapping, where low backscatter and low interferometric phase correlation indicate water regions.

Fuzzy set classification logic has been introduced to address the challenges of representing natural object boundaries in satellite images. This logic considers the heterogeneous and imperfect nature of the real world, assigning each pixel multiple membership values associated with the degree of correlation with different classes. Subpixel mapping technology, utilizing spatial correlation principles, aims to increase the spatial resolution of fuzzy classification results.

Despite these advancements, challenges persist in accurately extracting flood-affected areas from SAR imagery. Issues include the relationship between radar wavelength and terrain roughness, especially in windy conditions creating ripples on water surfaces. Forest cover poses difficulties in identifying inundated

areas, and the high backscatter from buildings within settlements can overlay floodwater backscatter. The orientation of rough surfaces and the directional nature of radar signals also contribute to varied tonal signatures, making it challenging to establish universal threshold values for flood detection. Regional knowledge and extensive field surveys remain crucial in setting effective threshold values for SAR image interpretation.

Chapter 3

Study Area

3.1 Location

Delhi, the capital city of India, is located in the northern part of the country. It is situated on the west bank of the Yamuna River and is surrounded by the states of Haryana and Uttar Pradesh. The geographical coordinates of Delhi are approximately between 28.6139°N latitude and 77.2090°E longitude. The city is known for its rich history, diverse culture, and strategic importance, serving as a political, cultural, and commercial hub in India. The National Capital Territory (NCT) of Delhi includes Old Delhi and New Delhi, with New Delhi serving as the seat of all three branches of the Government of India.

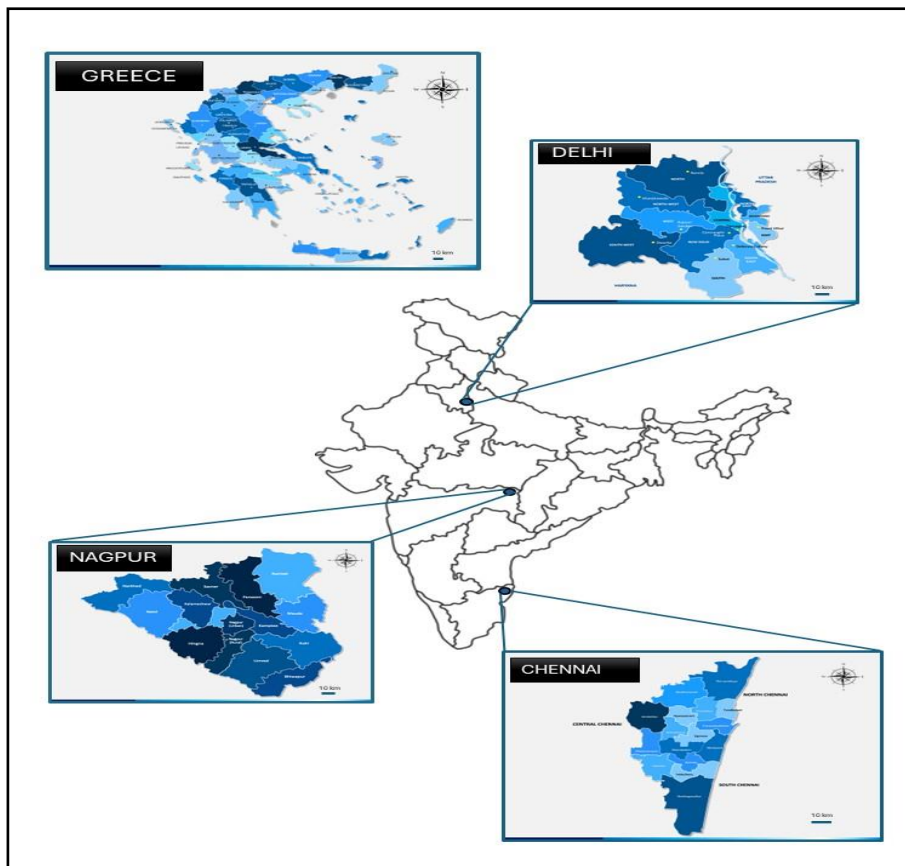


Fig 1: Location of study

3.2 Physiography and Geomorphology

Here is an overview of the physiography and geomorphology of the four study areas, with a focus on their relevance to flood inundation:

Delhi, India:

Physiography: Delhi is located in the northern part of India, situated on the Indo-Gangetic Plain. The city is bordered by the Aravalli Range to the west and the Yamuna River to the east. The terrain is generally flat with some undulating features.

Geomorphology: The Yamuna River plays a significant role in the geomorphology of the region, flowing through the eastern part of the city. Floodplain areas along the Yamuna are particularly prone to inundation during heavy rains or when the river overflows. Additionally, human development has led to the loss of natural drainage, exacerbating the risk of flooding.

Chennai, India:

Physiography: Chennai is situated on the southeastern coast of India, bordering the Bay of Bengal. The city lies on a coastal plain and is surrounded by rivers such as the Adyar and Cooum, as well as numerous lakes and marshlands.

Geomorphology: The coastal location and the presence of multiple water bodies make Chennai particularly vulnerable to flooding, especially during the monsoon season. Low-lying areas and the encroachment of wetlands for urban development increase the risk of flood inundation.

Nagpur, India:

Physiography: Nagpur is located in the central part of India, in the state of Maharashtra. The city is situated in the Deccan Plateau region, with a topography that includes low hills and plains.

Geomorphology: Nagpur's landscape includes rivers such as the Nag and Pili

rivers, as well as numerous lakes. The combination of natural water bodies and urban development can lead to localized flooding during heavy rains. Poor drainage and changes in land use can exacerbate the risk of flooding.

Greece:

Physiography: Greece is a country with varied topography, including mountains, valleys, and coastal plains. The study area may encompass regions such as the Athens metropolitan area or other coastal cities, which are prone to different types of flooding.

Geomorphology: Coastal areas in Greece, such as Athens and other cities, are at risk of flooding due to the proximity to the sea and the potential for storm surges during severe weather. Rivers flowing through these areas can also contribute to flood risk, particularly in low-lying and densely populated areas.

In all four study areas, urban development and changes in land use have altered natural drainage patterns, increasing the potential for flood inundation. Understanding the physiography and geomorphology of these regions is crucial for accurate flood mapping and mitigation strategies.

3.3 Drainage Network and Sub-basin

The drainage network and sub-basins in Delhi play a crucial role in managing water flow and addressing issues related to flooding.

3.3.1 Drainage Network:

Delhi's drainage system consists of a network of natural and artificial drains, canals, and rivers that facilitate the efficient disposal of rainwater and wastewater. The primary drainage features include:

Yamuna River: The Yamuna, a major river, flows along the western border of Delhi. It serves as a natural drainage outlet for the

Natural Drains: Delhi has several natural drains, such as the Najafgarh Drain, Supplementary Drain, Barapullah Drain, and others, which help in channeling rainwater away from urban

Artificial Drains: To cope with urbanization and increased impervious surfaces, Delhi has an extensive network of artificial drains and stormwater channels designed to prevent

3.3.2 Sub-Basins:

Delhi is divided into several sub-basins, each contributing to the overall drainage patterns. Some of the notable sub-basins include:

Yamuna Sub-Basin: Encompassing the areas along the Yamuna River, this sub-basin is critical for managing the water flow along the river.

Najafgarh Basin: The Najafgarh Drain, a significant natural drain, is part of this basin. It plays a vital role in draining excess water from the southwestern parts of Delhi.

Sahibi Basin: This basin includes areas that contribute to the Sahibi River, impacting the overall drainage dynamics in the region.

Understanding the drainage network and sub-basins is essential for effective urban planning, flood management, and infrastructure development in Delhi. It allows authorities to identify vulnerable areas, implement drainage improvements, and mitigate the impact of heavy rainfall events.

3.4 Climate

Delhi, India:

Situated in northern India, Delhi experiences extreme weather variations. The summer months, spanning from March to June, bring scorching heat, with temperatures often surpassing 40°C. Monsoons arrive in July, offering relief but are often accompanied by irregular and insufficient rainfall, exacerbating water

scarcity issues. Winters, lasting from November to February, are relatively cool, with occasional temperatures dropping below 5°C. During this period, the city grapples with fog, a phenomenon worsened by air pollution stemming from rapid urbanization, vehicular emissions, and industrial activities. Addressing these environmental challenges demands sustainable solutions and proactive measures, considering Delhi's dynamic and expanding urban landscape.

Chennai, India:

Chennai, located in southern India, experiences a tropical climate characterized by high temperatures and distinct wet and dry seasons. The summer months, from March to June, bring intense heat, with temperatures soaring above 40°C. Monsoons typically arrive in July, providing relief but often resulting in erratic and insufficient rainfall, leading to water scarcity concerns. Winters are milder, with temperatures ranging from 20°C to 25°C. Chennai also faces environmental challenges, including water pollution and urban sprawl, necessitating sustainable approaches to address these issues amidst the city's rapid growth.

Nagpur, India:

Nagpur, situated in central India, experiences a subtropical climate with significant temperature variations throughout the year. Summers, spanning from March to June, are hot and dry, with temperatures exceeding 40°C. Monsoons arrive in July, bringing relief but also contributing to waterlogging issues due to heavy rainfall. Winters, lasting from November to February, are cooler, with temperatures occasionally dropping below 5°C. Nagpur faces environmental challenges such as air and water pollution, exacerbated by rapid industrialization and urbanization. Addressing these concerns requires integrated strategies focusing on sustainable development and environmental conservation.

Greece:

Greece, located in southeastern Europe, exhibits diverse climatic conditions influenced by its geographical features. Summers, from June to August, are hot

and dry, with temperatures frequently exceeding 30°C. Winters, lasting from December to February, are milder, with temperatures ranging from 5°C to 15°C. Greece experiences distinct wet and dry seasons, with rainfall concentrated mainly in the winter months. The country faces environmental challenges such as deforestation, soil erosion, and water pollution, compounded by factors like agricultural practices and tourism. Sustainable management of natural resources and conservation efforts are essential to address these environmental concerns and ensure the preservation of Greece's unique ecosystems.

3.5 Soil and vegetation

Delhi, India:

Delhi's soil composition and vegetation are influenced by its location and rapid urbanization. The region predominantly features alluvial soil, fertile sediment deposited by the Yamuna River, supporting agricultural activities. However, extensive urban development has significantly reduced arable land in the area. The vegetation in Delhi comprises a blend of native and introduced species. Parks and green spaces boast a variety of trees, including neem, peepal, banyan, and mango. Despite this diversity, urbanization and pollution pose significant stress on the city's greenery. Efforts to promote afforestation and preserve green belts are crucial for maintaining ecological balance and enhancing the overall environmental quality of Delhi.

Chennai, India:

Chennai's soil composition and vegetation are shaped by its coastal location and urban expansion. The region's soil is primarily sandy, influenced by its proximity to the Bay of Bengal. This type of soil limits agricultural opportunities but supports coastal vegetation like palm trees and casuarinas. Chennai's vegetation includes a mix of native and introduced species, with parks and green spaces showcasing trees such as coconut palms, banyans, and tamarind. However, urbanization and industrialization have led to the depletion of green cover and encroachment on natural habitats, emphasizing the need for conservation efforts

to protect Chennai's biodiversity and ecological balance.

Nagpur, India:

Nagpur's soil composition and vegetation are influenced by its central location and agricultural heritage. The region predominantly features black cotton soil, known for its high fertility but susceptibility to waterlogging and erosion. This soil type supports crops like cotton, soybeans, and pulses. Nagpur's vegetation includes a mix of forested areas, grasslands, and urban greenery. Native species such as teak, sal, and bamboo are prevalent, along with fruit-bearing trees like mango and guava. However, urbanization and deforestation pose challenges to the region's green cover and ecological health, underscoring the importance of sustainable land management practices and conservation efforts.

Greece:

Greece's soil composition and vegetation vary across its diverse landscape, influenced by its Mediterranean climate and geological features. The country's soil types range from rocky and infertile in mountainous regions to fertile and clayey in valleys and plains. These soils support a variety of vegetation, including olive trees, citrus fruits, vineyards, and aromatic herbs like thyme and oregano. Forests of pine, cypress, and oak are also prominent in certain regions. However, factors such as deforestation, wildfires, and land degradation pose threats to Greece's soil quality and biodiversity. Sustainable land management practices and conservation initiatives are essential to safeguard Greece's unique ecosystems and agricultural heritage.

3.6 Economic Aspect

Delhi, India:

Delhi, the bustling capital of India, stands as a formidable economic powerhouse with a multifaceted economy. The service sector reigns supreme, encompassing industries such as information technology, telecommunications, and financial services, contributing significantly to the city's economic vitality.

Moreover, Delhi's stature as the political center of India amplifies its economic importance, attracting government institutions and administrative offices. The city's industrial zones are bustling hubs fostering diverse manufacturing activities, further diversifying its economic base. Vibrant markets and a thriving tourism sector add vibrancy to Delhi's economic landscape, catering to both domestic and international visitors. Educational institutions play a crucial role in nurturing a skilled workforce, complemented by ongoing infrastructure initiatives aimed at enhancing connectivity and efficiency. The real estate and construction sectors are integral components, meeting the demands of a burgeoning population and fueling urban development. This economic dynamism positions Delhi as a hub for opportunities and growth, essential for strategic planning and development initiatives aimed at sustaining its economic momentum.

Chennai, India:

Chennai, a bustling metropolis in southern India, boasts a diverse and dynamic economy driven by various sectors. The service industry, comprising information technology, telecommunications, and financial services, forms the backbone of Chennai's economy, leveraging its skilled workforce and technological infrastructure. Additionally, Chennai's status as a prominent manufacturing hub contributes significantly to its economic prowess, with industries such as automobile manufacturing, electronics, and textiles thriving in the region. The city's bustling markets and burgeoning tourism sector further add to its economic vibrancy, attracting visitors and fostering commercial activities. Educational institutions play a vital role in supplying a skilled workforce, while ongoing infrastructure projects enhance connectivity and support economic growth. The real estate and construction sectors cater to the city's growing population, fueling urban development and infrastructure expansion. Chennai's diverse economic landscape positions it as a hub for innovation, entrepreneurship, and economic growth in India.

Nagpur, India:

Nagpur, located in central India, boasts a diverse and thriving economy supported by various sectors. The city's industrial zones are key contributors, hosting various manufacturing activities including textiles, metals, and engineering goods. Additionally, Nagpur's strategic location and well-developed infrastructure make it a significant logistics and transportation hub, facilitating regional trade and commerce. The service sector, encompassing information technology, telecommunications, and financial services, also plays a vital role in driving Nagpur's economic growth, leveraging its skilled workforce and technological capabilities. The city's vibrant markets and emerging tourism sector further contribute to its economic vibrancy, attracting visitors and stimulating commercial activities. Educational institutions in Nagpur provide a skilled workforce, while ongoing infrastructure projects support economic development and urban expansion. The real estate and construction sectors are integral components, meeting the needs of a growing population and fueling urbanization. Nagpur's diverse economic landscape positions it as a center for opportunities and growth in central India, essential for its continued prosperity and development.

Greece:

Greece, a country with a rich cultural heritage and strategic geographical location, boasts a diverse and resilient economy. The service sector, including tourism, shipping, and financial services, serves as a cornerstone of Greece's economy, capitalizing on its natural beauty, historical sites, and maritime resources. Additionally, Greece's manufacturing sector, encompassing industries such as food processing, pharmaceuticals, and machinery, contributes significantly to its economic output, leveraging its skilled workforce and competitive advantages. Agriculture, although less prominent, remains an essential component of Greece's economy, with products like olives, grapes, and dairy products being major exports. The real estate and construction sectors play a crucial role in meeting the housing and infrastructure needs of both residents

and tourists, supporting economic growth and development. Educational institutions and ongoing infrastructure projects further contribute to Greece's economic resilience, fostering innovation, entrepreneurship, and skills development. Despite challenges, Greece's diverse economic landscape positions it as a dynamic and attractive destination for investment and business opportunities, vital for its sustainable growth and prosperity.

3.7 Demography

Delhi, India's bustling capital, is a melting pot of diverse demographics, reflecting the country's rich cultural tapestry. With a population surpassing 30 million, the city stands as one of the most populous globally. Its demographic makeup is characterized by a mix of various ethnicity, religions, and languages.

The city's demographic landscape is dynamic, shaped by a steady influx of people from different parts of India seeking economic opportunities, education, and a vibrant urban lifestyle. This migration contributes to the city's cosmopolitan identity, fostering a unique blend of traditions and modernity.

Delhi's demographic diversity is evident in its neighbourhoods, each with its distinct cultural nuances. From historic Old Delhi to the modernity of New Delhi, the city accommodates a spectrum of communities coexisting in a dynamic urban setting.

Education and employment opportunities further attract a young demographic, making Delhi a hub for students and professionals alike. The demographic tapestry, constantly evolving, adds to the city's energy and vitality, encapsulating the essence of India's demographic mosaic.

3.8 Road Networks

Delhi's extensive road network is a lifeline for the city's dynamic activities, connecting neighborhoods with local roads and enabling seamless travel through

arterial routes. The iconic Ring Road, both inner and outer, serves as a critical link, encircling the heart of Delhi. National Highways like NH1, NH2, and NH8 radiate from the city, connecting it to far-reaching destinations.

Expressways like the Yamuna Expressway, cutting travel time to Agra, and the Delhi-Gurgaon Expressway, a vital link to Gurugram, contribute to the efficiency of the network. The DND Flyway acts as a swift connection between Delhi and Noida.

These roadways are not just conduits for commuting; they shape the economic landscape, fostering trade and commerce, while also knitting together the social fabric of the city. Delhi's roads are more than mere thoroughfares; they are the veins and arteries of a pulsating metropolis, facilitating its continuous growth and vibrancy.

3.9 Canal Network

The river Yamuna passes through the eastern parts of Delhi, and water flowing in the Delhi segment of the river is obtained by the city government for treatment and distribution to citizens. The volume of water available in the river varies during the year. During the two to three months of the rainy season (July to September), the water level is high.

The upper Ganga canal, originating from the Ganga River at Haridwar in Uttarakhand, passes through Uttar Pradesh (UP) and serves both irrigation and drinking water purposes. It comes closest to Delhi at Muradnagar in UP, where infrastructure connects the canal water to Delhi.

Two key canals from Haryana, the Western Yamuna Canal (WYC) and Munak Canal, provide crucial water sources to the north of Delhi. Originating from the Yamuna River, they play a vital role in Delhi's water supply. However, challenges like inadequate water supply and pollution, including disruptions in 2016 due to local protests damaging canal infrastructure, have been noted.

The third external source for Delhi's water is the Bhakra storage in Himachal Pradesh, receiving waters from the Ravi and Beas rivers. A link canal connects Bhakra Canal to the Western Yamuna Canal (WYC). After reaching Haryana, the water is conveyed to Delhi through the WYC and Munak Canal.

River Yamuna flows through Delhi for a stretch of 22 kms from Wazirabad to Okhla barrage and its spread varies from 1.5 km to 3 km. Total River bed/flood prone area is around 97 sq.km, which is about 7% of the total area of Delhi. The river extends beyond its channel into the city.

Chapter 4

Material and Methods

To conduct any research, diverse data types are essential, sourced from various channels and serving distinct purposes. This chapter provides a concise overview of the input data, specifically the SENTINEL images utilized for extracting flooded areas. It also outlines key characteristics of SENTINEL, including its orbit, system specifications, SAR antenna details, and the available beam modes. The chapter delves into the backscatter coefficient values of SAR images and their generation. Understanding and considering these pre-processing steps is vital during data processing, result analysis, and drawing conclusions. Finally, the chapter outlines a brief methodology illustrating how the input data is employed in various techniques to generate flood inundation maps.

4.1 Introduction to SENTINEL

The SENTINEL-1 mission is the European Radar Observatory for the Copernicus joint initiative of the European Commission (EC) and the European Space Agency (ESA). Copernicus is a European initiative for the implementation of information services dealing with environment and security. It is based on observation data received from Earth Observation satellites and ground-based information.

The SENTINEL-1 mission includes C-band imaging operating in four exclusive imaging modes with different resolution (down to 5 m) and coverage (up to 400 km). It provides dual polarisation capability, very short revisit times and rapid product delivery. For each observation, precise measurements of spacecraft position and attitude are available.

Synthetic Aperture Radar (SAR) has the advantage of operating at wavelengths not impeded by cloud cover or a lack of illumination and can acquire data over a site during day or night time under all weather conditions. SENTINEL-1, with its [C-SAR instrument](#), can offer reliable, repeated wide area monitoring.

4.1.1 The SENTINEL orbit

SENTINEL-1 is in a near-polar, sun-synchronous orbit with a 12 day repeat cycle and 175 orbits per

cycle for a single satellite. Both SENTINEL-1A and SENTINEL-1B share the same orbit plane with a 180° orbital phasing difference. With both satellites operating, the repeat cycle is six days.

In particular for interferometry, SENTINEL-1 requires stringent orbit control. Satellite positioning along the orbit must be accurate, with pointing and timing/synchronisation between interferometric pairs. Orbit positioning control for SENTINEL-1 is defined using an orbital Earth fixed "tube", 50 m (RMS) wide in radius, around a nominal operational path. The satellite is kept inside this "tube" for most of its operational lifetime.

4.1.2 SENTINEL System Specifications

Parameter	Value
Frequency Range	C-band (Approximately 4 to 8 GHz)
Wavelength	3.75 cm to 7.5 cm
RF Bandwidth	Variable (Depends on Operational Mode)
Antenna Size	Specific to SAR Mode and Design

Table 1: Sentinel Specifications

4.1.3 SAR Antenna

Specification	Details
Antenna Type	Phased-Array
Frequency	C-band
Wavelength	~3.5 cm
RF Bandwidth	Broadband

Antenna Size	Electronically Steerable
Polarization Modes	Dual-Polarization (HH, VV), Interferometric
SAR Modes	Stripmap, Interferometric Wide Swath, Extra Wide Swath, Wave
Coverage and Resolution	Variable, depending on SAR mode
Repeat cycle	Short revisit times as part of a satellite constellation

Table 2: Sentinel antenna specifications

4.1.4 SENTINEL Beam Modes

SENTINEL-1 operates in four exclusive [acquisition modes](#):

1. Stripmap (SM)
2. Interferometric Wide swath (IW)
3. Extra-Wide swath (EW)
4. Wave mode (WV)

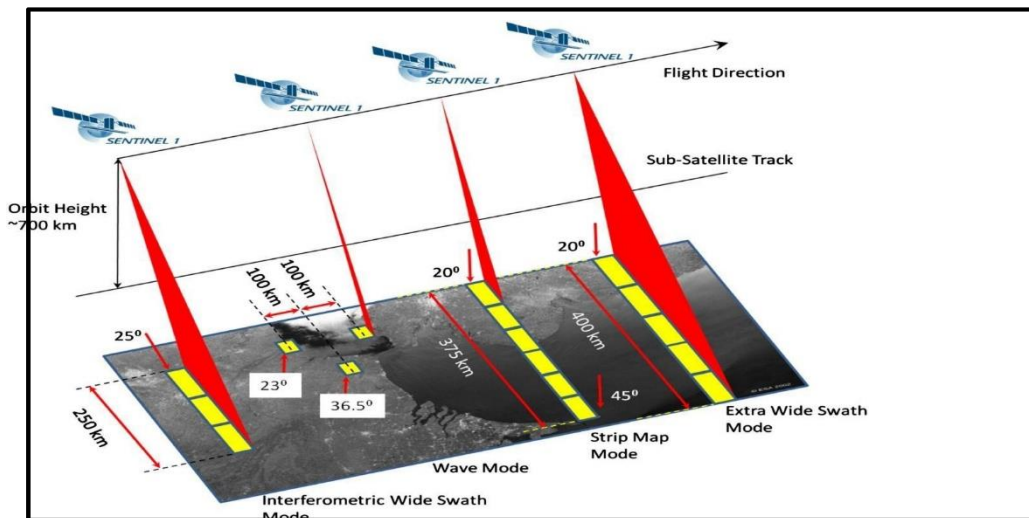


Fig 2: Acquisition modes

4.2 SENTINEL Data Products

Each mode can potentially produce products at SAR Level-0, Level-1 SLC, Level-1 GRD, and Level-2 OCN.

Data products are available in single polarisation (VV or HH) for Wave mode and dual polarisation (VV+VH or HH+HV) or single polarisation (HH or VV) for SM, IW, and EW modes.

The SAR [Level-0 products](#) consist of the sequence of Flexible Dynamic Block Adaptive Quantization (FDBAQ) compressed unfocused SAR raw data. For the data to be usable, it will need to be decompressed and processed using a SAR processor.

Level-1 data consists of Single Look Complex (SLC) and Ground Range Detected (GRD) products. SLC products provide geo-referenced SAR data in slant-range geometry, preserving phase information. GRD products, on the other hand, have detected, multi-looked, and ground-range projected data, with loss of phase information. GRD comes in Full Resolution (FR), High Resolution (HR), and Medium Resolution (MR), depending on the amount of multi-looking performed. These products cater to different spatial resolutions and speckle reduction needs.

Level-2 Ocean (OCN) products consist of Ocean Swell spectra (OSW), Ocean Wind Fields (OWI), and Surface Radial Velocities (RVL). OSW provides a two-dimensional ocean surface swell spectrum with wind speed and direction estimates. It's generated from Stripmap and Wave modes. OWI offers a ground range gridded estimate of surface wind speed and direction at 10 m, derived from Level-1 GRD images of SM, IW, or EW modes. RVL represents the difference between the measured Level-2 Doppler grid and the Level-1 calculated geometrical Doppler, providing valuable oceanographic information.

4.3 Pre-Processing of Sentinel data

A standardized preprocessing workflow for Copernicus Sentinel-1 GRD data is outlined, tailored for the Sentinel application platform (SNAP). The workflow, available in XML format on GitHub, consists of seven steps:

1. Apply Orbit File: Corrects inaccurate orbit state vectors in product metadata by applying precise orbits from SNAP.
2. Thermal Noise Removal: Reduces additive thermal noise in Sentinel-1 image intensity, enhancing

data quality.

3. **Border Noise Removal:** Corrects radiometric artifacts caused by azimuth and range compression at image borders.
4. **Calibration:** Converts digital pixel values to radiometrically calibrated SAR backscatter using a calibration vectors.
5. **Speckle Filtering:** Applies speckle filtering, reducing granular noise to enhance image quality.
6. **Range Doppler Terrain Correction:** Compensates for geometric distortions due to side-looking geometry, using a digital elevation model for correlation.
7. **Conversion to dB:** Logarithmically transforms the unitless backscatter coefficient to dB for the final product.

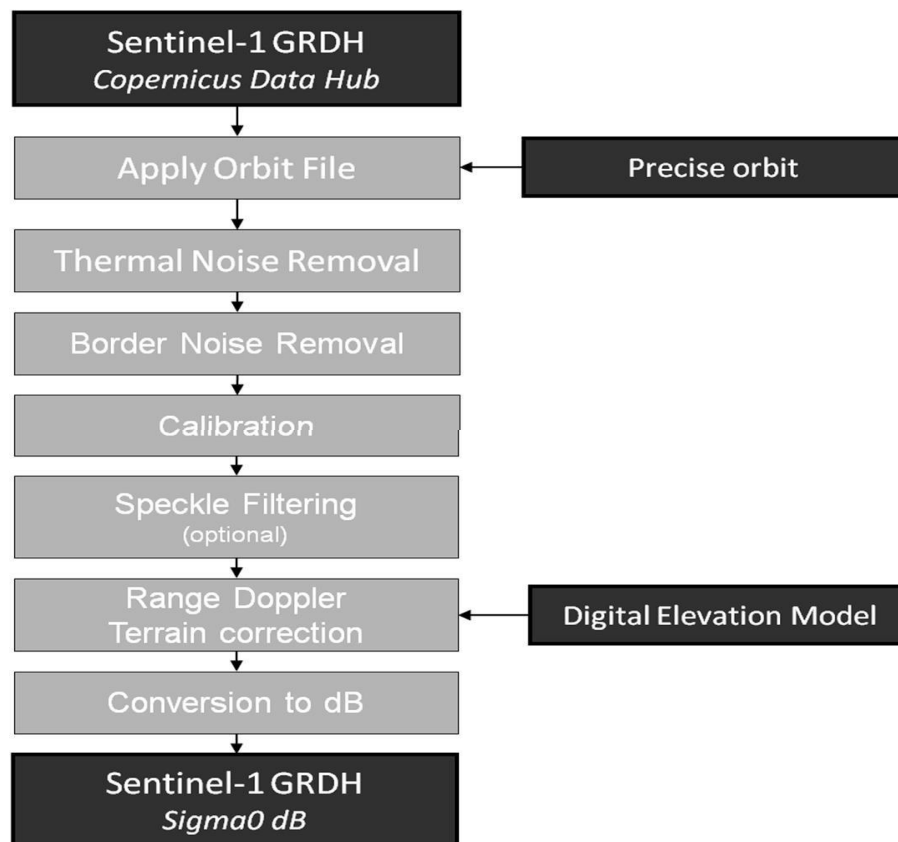


Fig 3: Sentinel-1 Ground Range Detected (GRD) preprocessing workflow.

4.4 Overall Methodology

and Software used

The study employs a remote sensing methodology, specifically utilizing four classification techniques on gSENTINEL 1 GRD data to delineate flood extent. While visual interpretation offers accuracy, it is labor-intensive and time-consuming. On the other hand, the threshold technique, widely utilized for its speed, relies solely on backscatter coefficient values, which can be influenced by factors such as tree canopy, agricultural fields, and human-made structures, potentially affecting the precision of flood map generation.

The methodology for mapping and analyzing flood inundation in Delhi using Sentinel-1 SAR data involves a systematic process. Initially, Sentinel-1 GRD data is collected, filtering based on specific parameters such as mode, polarization, orbit, and resolution. The data undergoes preprocessing, including temporal and speckle filtering using the Refined Lee filter. Flood detection is performed by calculating the ratio between filtered SAR images before and after flood events. A threshold is then applied to identify flooded areas, and masks for permanent water and slope are utilized to refine the flood extent. Connectivity analysis removes disconnected areas, and the processed layers, including the initial flood extent and relevant masks, are visualized. Area calculations are conducted, determining the total district area and the area of identified flooded zones. The results, along with quality assurance and acknowledgment of limitations, are exported to Google Drive in CSV format. The methodology concludes with a summary of steps, key findings, and suggestions for future work.

There are various image processing software for processing and analysis of remotely sensed datasets. In the present work, Google Earth Engine has been used for on-screen digitization resulting in the generation of the flood inundated areas. The results were then visualized in the Qgis. The python was also used to get some statistics of the data.

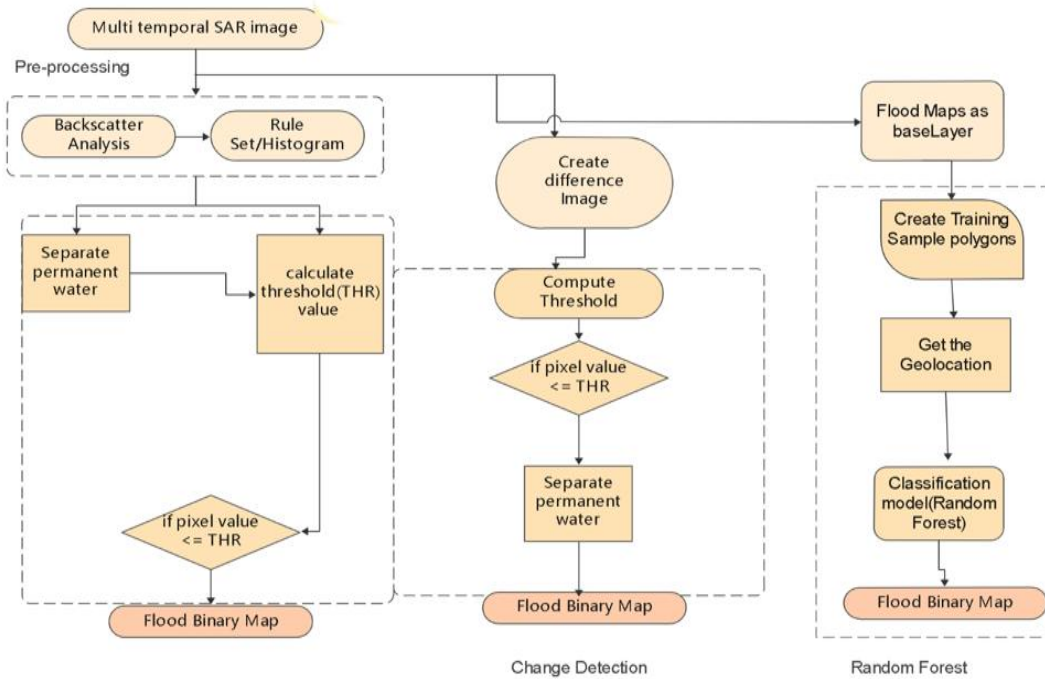


Fig 4: Flowchart for methodology

4.5 Extraction of flooded areas

4.5.1 Data used for monitoring Delhi floods

In July 2023, heavy rainfall triggered severe flooding across Northern India, including the national capital of Delhi. The unprecedented monsoon rains, exceeding normal rainfall by over 150%, caused the Yamuna River, which flows through Delhi, to breach its danger mark by over 4 meters. The floods caused widespread damage to property and infrastructure, and displaced thousands of people. The river breached its danger mark on July 13, and the floods reached their peak on July 14. The water levels started to recede on July 15, and the floods were largely subsided by July 17.

The Delhi floods of 2023 occurred in two distinct phases:

Phase 1: July 9-16, 2023

The initial flooding event began on July 9, 2023, as heavy rainfall over 153 millimeters (6.0 inches) in a single day caused the Yamuna River to cross its danger mark. This led to extensive flooding in low-lying

areas, particularly near the riverbanks. The floods continued for several days, with the Yamuna River reaching its highest level in over 45 years on July 13, 2023.

Phase 2: August 12-13, 2023

Parameter	Value/Description
Location	Delhi
Date Range (Before)	June 15, 2023 to June 30, 2023
Date Range (After)	July 1, 2023 to July 30, 2023
Flood Dates	June 18, 2023; June 30, 2023; July 12, 2023; July 24, 2023
SAR Data Source	Copernicus Sentinel-1
SAR Instrument Mode	Interferometric Wide (IW)
Polarization	Vertical Transmit, Vertical Receive (VH)
Orbit Properties	Descending
Resolution	10 meters
Speckle Filtering	Refined Lee Speckle Filter
Threshold	1.25 (for flood detection)
Additional Filters	Permanent/Semi-permanent water, slope, and connected pixels
Result Output	Flooded areas in hectares

Table 3: Representation of key elements related to the Algorithm and Data used

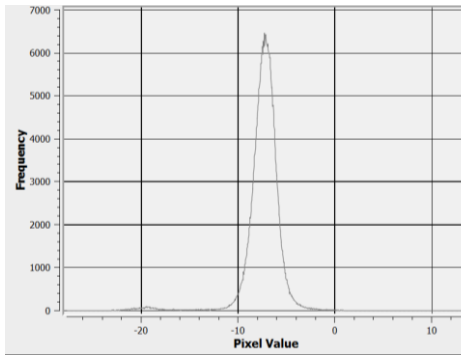
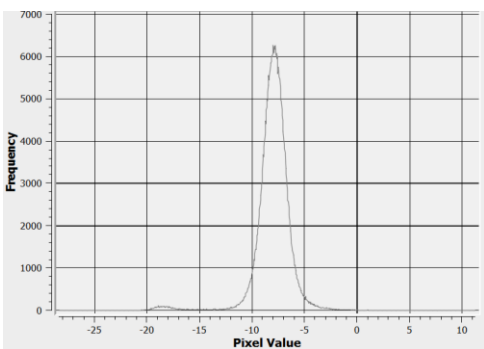
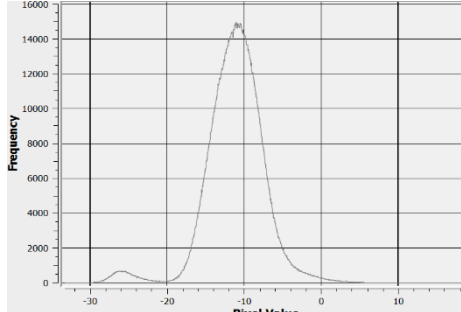
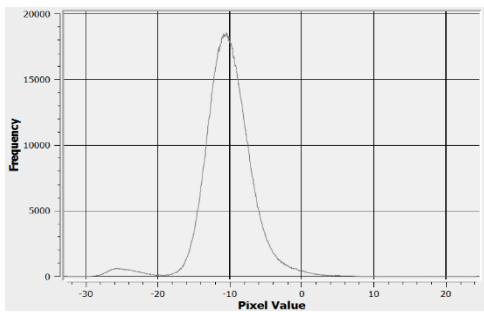
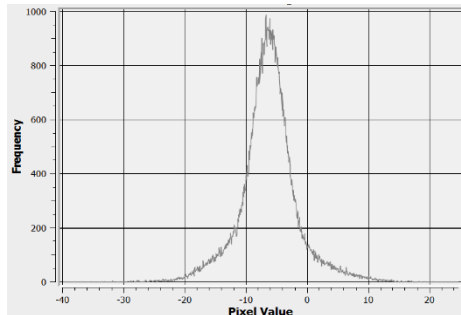
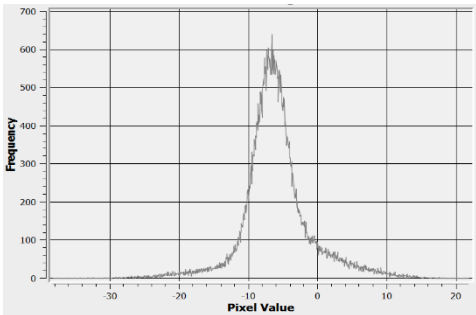
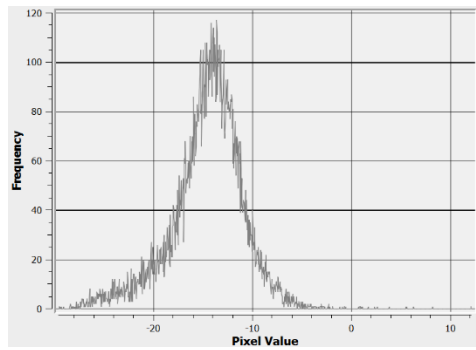
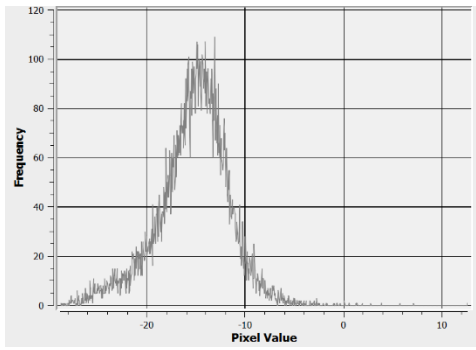


Fig 5: Histogram Before/After (Delhi, Chennai, Nagpur, Greece)

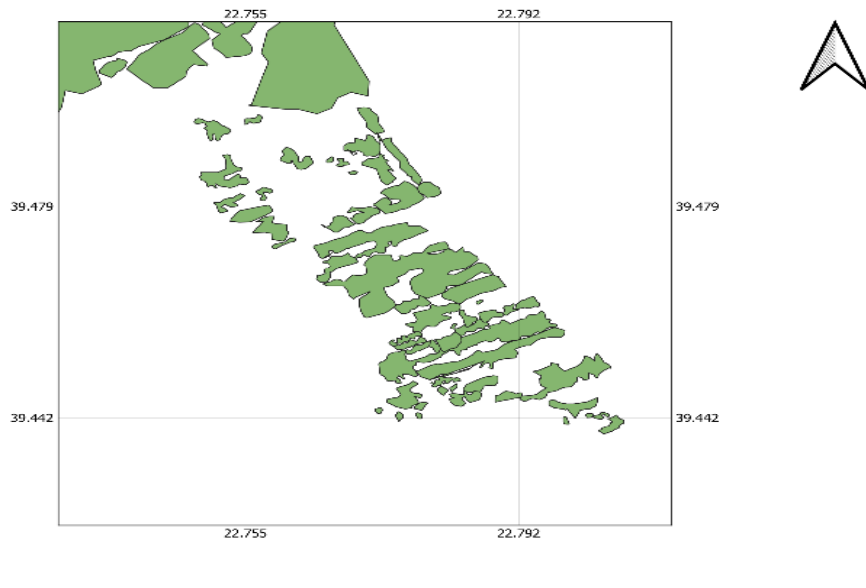
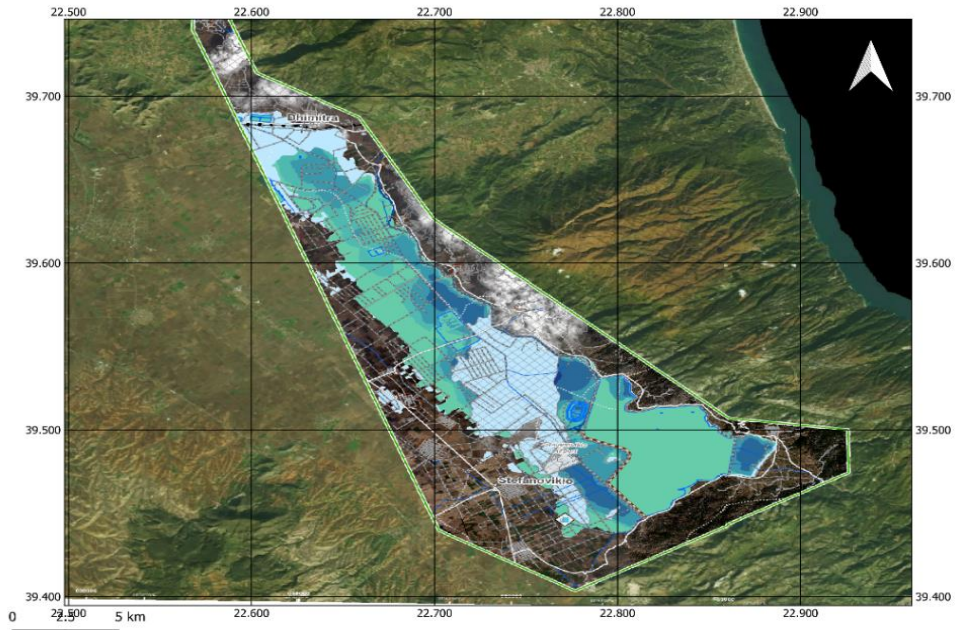


Fig 6: Reference Flood Map/Sample training data

4.5.2 Flooded Area

The flooded area in the provided code is computed through a multi-step process involving Synthetic Aperture Radar (SAR) image analysis. Initially, the script calculates the ratio between pre-flood and post-flood SAR images, identifying areas of significant change. A threshold is then applied to this ratio image to establish an initial flooded area mask. Subsequent steps refine this mask by excluding permanent water bodies and areas with steep slopes. Isolated pixels are removed to enhance the continuity of flooded regions. The final calculation involves measuring the flooded area within a specified district using pixel-wise area computations. The results, including the total district area and the flooded area in hectares, are exported to a CSV file for further analysis. This comprehensive approach provides a quantitative assessment of the extent of flooding in the designated region.

In the provided algorithm, the threshold value is set to 1.25. This threshold is applied to the ratio image derived from the division of post-flood and pre-flood Synthetic Aperture Radar (SAR) images. The choice of this threshold is a crucial step in flood detection. It essentially determines the sensitivity of the algorithm in identifying flooded areas. A higher threshold results in a more conservative flood extent, highlighting only the most significant changes. On the other hand, a lower threshold may include more subtle changes but could lead to the inclusion of false positives. The specific value of 1.25 is likely determined through experimentation and validation to strike a balance between sensitivity and accuracy based on the characteristics of the SAR data and the study area. Adjusting this threshold might be necessary depending on the specific conditions of the study region and the desired trade-off between false positives and false negatives.

4.5.3 Rule Based Classification

Calculation of Backscatter Difference:

The backscatter difference (`difference``) is computed by dividing the post-flood backscatter (`afterFiltered``) by the pre-flood backscatter (`beforeFiltered``):

Thresholding for Flood Detection: The thresholding step involves comparing the backscatter difference (`difference``) with a predefined threshold value (`diffThreshold``). Pixels with a backscatter ratio above this threshold are considered indicative of flooded regions. This is represented by the following equation:

$$\mathit{flooded} = \mathit{difference} > \mathit{diffThresholdPermanent/Semi - permanent}$$

Water Masking: A mask (`permanentWater`) is applied to exclude areas with permanent or semi-permanent water. The Global Surface Water (GSW) dataset is used, where areas with a seasonality value greater than or equal to 5 are considered permanent water. The masking equation is:

$$\mathbf{flooded} = \mathbf{flooded} * (1 - \mathbf{permanentWater})$$

Masking Based on Slope: Areas with a slope greater than a specified threshold (`slopeThreshold`) are masked out. The masking equation is:

$$\mathbf{flooded} = \mathbf{flooded} * (\mathbf{slope} < \mathbf{slopeThreshold})$$

Isolated Pixel Removal: To remove isolated pixels, the connected pixel count (`connections`) is computed, and flooded pixels with connections below a specified threshold (`connectedPixelThreshold`) are excluded. The masking equation is:

$$\mathbf{flooded} = \mathbf{flooded} * (\mathbf{connection} > \mathbf{connectedPixelThreshold})$$

These equations collectively describe the process of flood detection, where the backscatter difference is thresholded, and subsequent masks are applied to refine the results.



4.5.4 Change Detection Technique

The algorithm follows a comprehensive change detection process to identify and map flooded areas based on backscatter values derived from synthetic aperture radar (SAR) data. Initially, the backscatter values for pre- flood and post-flood periods are computed, and these values are typically presented in decibels (dB) to enhance the visibility of subtle variations in the dynamic range.

The change detection process involves defining a threshold value, denoted as `diffThreshold` (set to 1.25 in the provided code), which serves as a critical indicator of significant changes in backscatter values. Pixels with change values above this threshold are considered as initial estimates of potentially flooded areas. This thresholding step is crucial for identifying regions undergoing substantial changes indicative of flooding.

To refine the flood detection and minimize false positives, the algorithm incorporates additional masking steps. Permanent or semi-permanent water areas are masked out by applying a mask based on a water seasonality index, such as `gsw.select('seasonality').gte(5)`. This step aims to distinguish between actual flooding events and consistently water-covered regions.

Moreover, the algorithm considers the topography of the area by masking out regions with more than 5 percent slope. The slope information is derived from the HydroSHEDS Digital Elevation Model (DEM), allowing the algorithm to exclude areas where flooding is less likely based on terrain characteristics.

To improve the accuracy of the results, isolated pixels are removed through a connected pixel count approach. Pixels that are not part of a connected region with a sufficient number of neighboring pixels (controlled by the `connectedPixelThreshold`) are filtered out. This step helps to eliminate noise and isolated artifacts in the flooded area identification.

4.6 Mask used in algorithm

4.6.1 Permanent Water Mask:

Purpose:

The permanent water mask serves the purpose of excluding regions with constant water presence, such as rivers, lakes, and reservoirs, from the flood detection process. These areas are less likely to be affected by short-term flood events.

Method:

The Global Surface Water (GSW) dataset is employed to create a permanent water mask. The GSW dataset provides information about the seasonality of surface water over an extended period. Pixels identified as having a consistent presence of water throughout the year are considered permanent water.

Implementation:

The algorithm uses the GSW dataset to mask out pixels identified as permanent water. This ensures that areas with known water bodies are not misclassified as flooded during the detection process.

4.6.2 Slope Mask:

Purpose:

The slope mask is applied to account for the topographic characteristics of the terrain. Areas with steep slopes are less likely to experience flooding, and thus, the slope mask helps in excluding such regions.

Method:

The HydroSHEDS Digital Elevation Model (DEM) is utilized to calculate the slope of the terrain. Slope is a measure of the steepness of the landscape, and areas with slopes exceeding a specified threshold are considered less susceptible to flooding.

Implementation:

Pixels with slopes greater than the defined threshold are masked out. This ensures that areas with significant inclines, where flooding is less probable, are excluded from the flood detection process.

4.6.3 Isolated Pixels Removal:

Purpose:

Isolated pixel removal aims to improve the coherency of identified flooded zones. It eliminates isolated or disconnected pixels that may result from noise or errors in the detection process.

Method:

Connected pixel count analysis is applied to identify clusters of pixels. Pixels with fewer connected neighbors than a specified threshold are considered isolated and are subsequently removed from the flooded area classification.

Implementation:

The algorithm removes isolated pixels based on the connected pixel count, which enhances the overall quality of the flood extent by ensuring that identified flooded areas are spatially coherent.

These masking techniques collectively enhance the accuracy of flood detection by excluding areas with known water bodies, considering topographic characteristics, and improving the overall coherence of the identified flooded zones. They contribute to creating a reliable and realistic representation of flood-affected areas in the Delhi district, providing valuable insights for further analysis and decision-making.

Why Mask Permanent/Semi-permanent Water?

The Global Surface Water dataset is a product developed by the European Commission's Joint Research Centre (JRC) in collaboration with Google. It provides information about the extent and dynamics of surface water bodies globally. The dataset is derived from multi-temporal satellite observations, primarily using the Sentinel-1 and Landsat missions.

Purpose of Using GSW in Flood Detection

The GSW dataset is leveraged in the algorithm to identify and mask out areas that are consistently

covered by water, regardless of the flood event. These areas are considered as permanent or semi-permanent water bodies. The rationale behind this step is to exclude regions that are naturally water-covered and not part of the flooded area during the specific flood event being analyzed.

4.7 Change Detection Technique

The algorithm follows a comprehensive change detection process to identify and map flooded areas based on backscatter values derived from synthetic aperture radar (SAR) data. Initially, the backscatter values for pre- flood and post-flood periods are computed, and these values are typically presented in decibels (dB) to enhance the visibility of subtle variations in the dynamic range.

The change detection process involves defining a threshold value, denoted as `diffThreshold` (set to 1.25 in the provided code), which serves as a critical indicator of significant changes in backscatter values. Pixels with change values above this threshold are considered as initial estimates of potentially flooded areas. This thresholding step is crucial for identifying regions undergoing substantial changes indicative of flooding.

To refine the flood detection and minimize false positives, the algorithm incorporates additional masking steps. Permanent or semi-permanent water areas are masked out by applying a mask based on a water seasonality index, such as `gsw.select('seasonality').gte(5)`. This step aims to distinguish between actual flooding events and consistently water-covered regions.

Moreover, the algorithm considers the topography of the area by masking out regions with more than 5 percent slope. The slope information is derived from the HydroSHEDS Digital Elevation Model (DEM), allowing the algorithm to exclude areas where flooding is less likely based on terrain characteristics.

To improve the accuracy of the results, isolated pixels are removed through a connected pixel count approach. Pixels that are not part of a connected region with a sufficient number of neighboring pixels (controlled by the `connectedPixelThreshold`) are filtered out. This step helps to eliminate noise and isolated artifacts in the flooded area identification.

4.8 Random Forest

Random Forest Classifier (RFC), an ensemble classifier, produces multiple decision trees using a subset of training samples and variables selected randomly. In the field of remote sensing, RFC provides an unbiased estimation of generalization error, can deal with a large number of variables, identifies missing data and the

outliers existing in the training samples, measures the correlation between data sets based on proximity , optimizes feature space by using the variable importance function , is relatively robust to outliers and noise. RF classifier has been used in many previous studies for land cover mapping, initially evaluating the performance of the RF classifier for classifying land cover in Spain, and their study achieved a higher overall accuracy (91%) compared to the single decision tree. In another study, Hayes et al. (2014) was able to prepare a high-resolution (1 m) land cover map in Wyoming using RF classifier and obtained an overall accuracy of 81%. To select the best classification model for land cover mapping in a complex farming area, an overall accuracy of 89% using RF classification. In some recent studies, the RF classification method has been undertaken for also generating flood inundation maps A study for urban flood mapping in China based on Unmanned Aerial Vehicle imagery and used an RF classifier for generating flood inundation maps. Results showed that the RF classifier outperformed (overall accuracy 87.3%) maximum likelihood classification and artificial neural network algorithms. In a recent study, they developed a framework for generating flood inundation maps based on SAR microwave remote sensing data and obtained an overall accuracy of 88.9% using an RF classifier. [1]



Fig 8: Chennai Flood 2023-Twitter

```
# Function to search tweets with images based on keyword, timespan, and location
def search_tweets(keyword, location, radius, start_date, end_date):
    # Convert the location coordinates to a geocode (latitude, longitude, radius in km)
    geocode = f"{location['latitude']},{location['longitude']},{radius}km"
```

```

# Main function
if __name__ == '__main__':
    # Define parameters
    keyword = '#ChennaiFlood' # Keyword to search for
    location = {
        'name': 'Chennai',
        'latitude': 13.0827,
        'longitude': 80.2707
    }

```

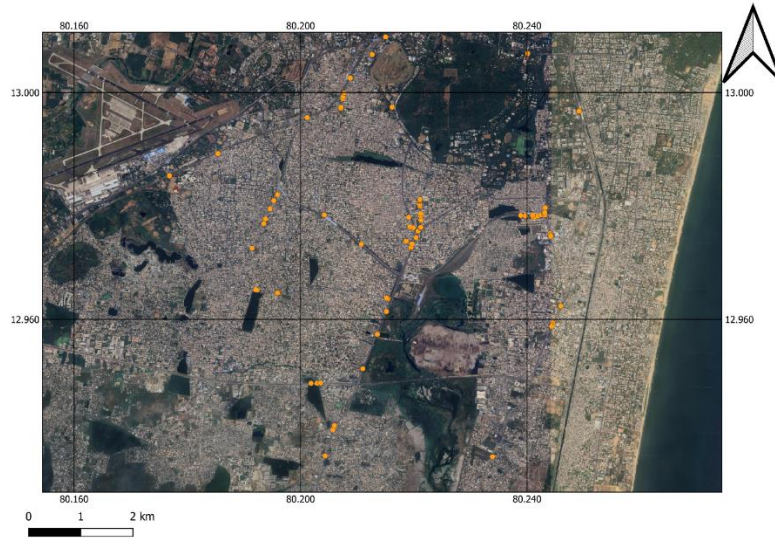


Fig 9: Crowd-sourced data – Social media

4.9 Methodology for Extracting Geotagged Social Media Flooded Pictures

The integration of social media data with traditional remote sensing techniques offers a powerful approach to enhancing flood mapping and monitoring efforts. Geotagged images from social media can provide real-time, ground-level observations that complement satellite-based data. This section details the methodology for extracting and utilizing geotagged social media images for flood mapping.

The first step in the process is selecting appropriate social media platforms that provide geotagged images. Popular platforms like Twitter, Instagram, and Flickr are often used because they allow users to share images with location metadata. Access to these platforms typically requires registering for developer access to obtain API keys. These keys are used to authenticate requests made to the platform's API, enabling

extracting relevant data.

4.9.1 Data Extraction

Once API access is secured, the next step involves defining search parameters. This includes selecting relevant keywords such as "flood," "inundation," "water level," and specific location names. It is also important to specify the geographic boundaries of interest using latitude and longitude coordinates and the time frame around the flood event. These parameters help filter the data to ensure relevance to the flood event being studied. Querying the API involves sending HTTP requests with these parameters and receiving responses, typically in JSON or XML format, which contain the details of the geotagged images.

4.9.2 Data Processing

After retrieving the data, it is necessary to parse the API responses to extract relevant information such as image URLs, geotags (latitude and longitude), timestamps, and any available user metadata. The data then undergoes filtering and cleaning to ensure quality and relevance. This step involves removing duplicate entries, filtering out low-quality images, and verifying the accuracy of geotags to eliminate erroneous data. Ensuring that the images are indeed flood-related can be done by checking associated text or tags.

4.9.3 Data Annotation

The cleaned and filtered data is then imported into Geographic Information System (GIS) software such as QGIS. This involves plotting the geotagged locations of the images on a map and overlaying these points on relevant geographic layers, including roads, rivers, and flood zones. Manual annotation of the images is carried out to confirm the presence of flooding. Each image is reviewed, and annotations such as "flood" or "no flood" are added based on visual inspection. Additional details like water depth, affected infrastructure, and the severity of the flooding can also be annotated if available.

4.9.4 Data Integration

To create a comprehensive dataset, a shapefile containing the geotagged and annotated images is created. This shapefile includes attributes such as image URL, coordinates, timestamp, and annotations, ensuring compatibility with other geospatial data formats used in the analysis. The social media data is then integrated with SAR data to enhance flood mapping efforts. This integration involves overlaying geotagged

images on SAR-based flood maps, allowing for validation and refinement of the flood classification. Ground-level observations from social media images help to improve the accuracy of the flood maps generated from SAR data.

4.9.5 Visualization and Analysis

Visualization of the geotagged and annotated images within the GIS software provides a clear representation of the flood extent. Maps are created to show the locations of flood-affected areas along with corresponding social media images. Different symbols or colors can be used to indicate the severity and type of flooding. This visual representation aids in analyzing spatial patterns of the flood event, identifying hotspots, and areas with high flood impact. Comparing the extent and severity of flooding observed from SAR data and social media images provides valuable insights for disaster management and response.

4.9.6 Data Collection and Preparation

The foundation of this flood mapping methodology is the collection of historical and current flood maps from reputable sources such as the National Remote Sensing Centre (NRSC) and the Indian Space Research Organisation (ISRO) in India, OpenStreetMap, and the Copernicus Emergency Management Service (CEMS). These maps provide critical base layers that inform the flood extent and are essential for accurate annotation and analysis.

4.9.7 Historical and Current Flood Maps

Flood maps from NRSC/ISRO provide detailed information on flood extents based on satellite imagery and other remote sensing data. OpenStreetMap offers user-generated geographical data that can include flood extents and related features. CEMS provides rapid mapping products for flood monitoring in Europe and globally. These sources are integrated into a Geographic Information System (GIS) environment, typically QGIS, to serve as base layers for further analysis.

4.9.8 Data Annotation

In the GIS environment, digital polygons are created to annotate the flood extent areas. This involves manually drawing polygons over the base maps to delineate areas affected by flooding. Each polygon is assigned an identifier: polygons representing flooded areas are given an ID of 1, while non-flooded areas are

assigned an ID of 0. This binary classification facilitates the supervised learning process. Once the annotation is complete, the data is exported as a shapefile, which includes the spatial information and the classification labels.

4.9.9 Supervised Classification with Random Forest

The supervised classification algorithm used in this methodology is the Random Forest classifier, a robust and versatile machine learning algorithm known for its accuracy and efficiency in handling large datasets with numerous features.

4.9.10 Feature Extraction

Before classification, relevant features are extracted from the SAR data and the annotated shapefiles. These features may include backscatter intensity values from pre- and post-flood SAR images, texture measures, and other derived indices that can help differentiate between flooded and non-flooded areas.

4.9.11 Training the Classifier

The Random Forest algorithm is trained using the annotated shapefile data. The training process involves feeding the algorithm with the features extracted from the SAR data along with the corresponding flood labels (1 for flood, 0 for no flood). The Random Forest classifier constructs multiple decision trees during training, with each tree voting on the classification outcome. The final classification is determined by aggregating the votes from all the trees.

4.9.12 Classification and Mapping

Once trained, the Random Forest classifier is applied to the entire study area to produce a flood map. The classifier analyzes the SAR data for the entire area and assigns a flood label to each pixel based on the learned patterns. This results in a detailed flood map highlighting the extent of flooding across the urban landscape.

4.9.13 Validation with Ground Truth Data

The accuracy of the flood map generated by the Random Forest classifier is validated using ground

truth data collected from social media. Geotagged images and reports from platforms like Twitter, Instagram, and Flickr are used as ground truth points. These images provide real-time, on-the-ground verification of flood conditions, which are crucial for validating the classification results.

4.9.14 Integration and Analysis

The ground truth data is integrated into the GIS environment, overlaying the geotagged social media images on the flood map. This allows for a visual and statistical comparison between the predicted flood extents and the actual flood observations. Areas of agreement between the flood map and the ground truth data indicate accurate classifications, while discrepancies highlight potential areas for further investigation and refinement of the model.

Chapter 5

Results

In the post-processing phase of flood detection using Google Earth Engine and subsequent analysis in QGIS, several key steps were undertaken to enhance the visual representation and interpretation of the results. The flood detection outcomes, initially identified through a thresholding process in Google Earth Engine, were exported as a CSV file and seamlessly integrated into QGIS for advanced geospatial analysis and mapping.

Upon importing the flood information into QGIS, the flooded areas were symbolized to facilitate a clear visual understanding. The use of a distinct color scheme, such as assigning a vivid red hue to the flooded regions, allowed for an immediate and intuitive identification of the impacted areas. This symbology not only provided clarity but also served as a foundational element for subsequent analyses.

To complement the flood detection results, additional contextual layers, including satellite imagery and administrative boundaries, were overlaid. This comprehensive approach facilitated a nuanced understanding of the spatial distribution of flood-affected zones within the broader geographic context. The iterative adjustment of layer styles, transparency settings, and label placements in QGIS contributed to the refinement of map visualizations, ensuring they effectively communicated the severity and extent of flooding.

A notable enhancement in the visual interpretation was achieved by incorporating the Global Surface Water dataset (gsw) to mask out areas with permanent or semi-permanent water bodies. This additional step, represented by a distinct blue color, aided in differentiating between flood-affected areas and pre-existing water bodies, thereby reducing the likelihood of misinterpretation.

Moreover, the use of a color palette, where permanent water bodies were assigned the color blue, facilitated a clearer distinction between natural water features and flood-induced water. This deliberate color choice contributed to a more nuanced and accurate visual representation, crucial for decision-making processes and the communication of results to diverse stakeholders.

In summary, the integration of Google Earth Engine flood detection results into QGIS, coupled with thoughtful symbology choices and the incorporation of contextual layers, significantly advanced the visual analysis of flood-affected areas. The utilization of a distinct blue color for permanent water bodies further

improved the interpretability of the results, enhancing the overall effectiveness of the mapping and analysis process.

5.1 Delhi Results

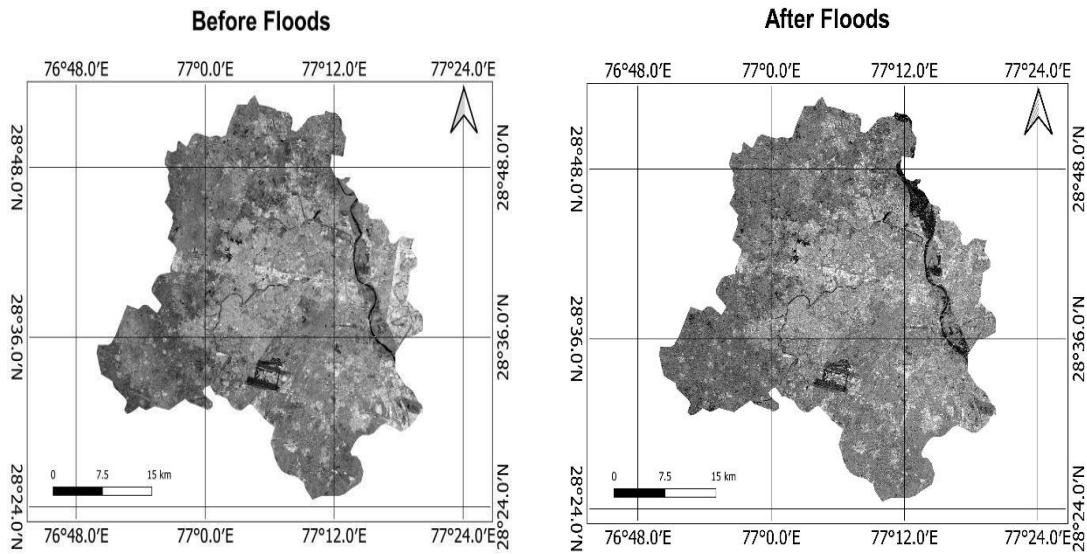
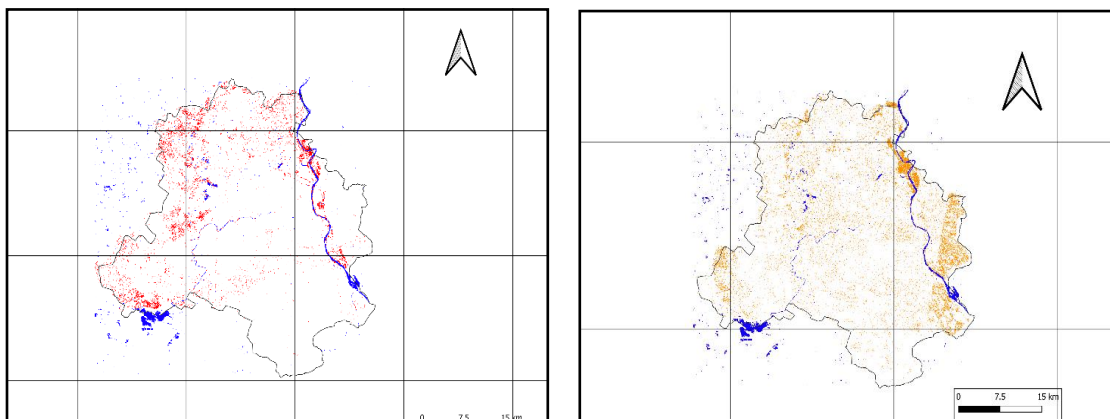


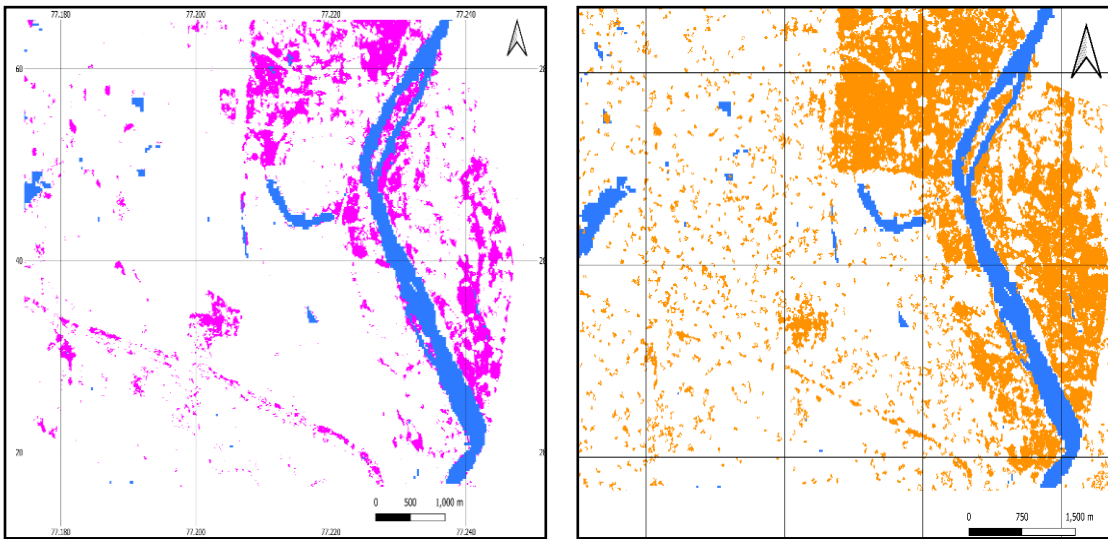
Fig 10: Filtered images of Delhi, before and after the flood



a)

b)

Fig 11: a) Rule based classification, and b) Change Detection



a)

b)

Fig 12: a) Rule-based classification, and b) Change detection

	precision	recall	f1-score	support
No Flood	0.78	0.37	0.50	102
Flood	0.33	0.74	0.46	43
accuracy			0.48	145
macro avg	0.55	0.56	0.48	145
weighted avg	0.64	0.48	0.49	145

precision	recall	f1-score	support	
0	0.22	0.04	0.07	130
1	0.81	0.97	0.88	546
accuracy			0.79	676
macro avg	0.51	0.50	0.47	676
weighted avg	0.69	0.79	0.72	676

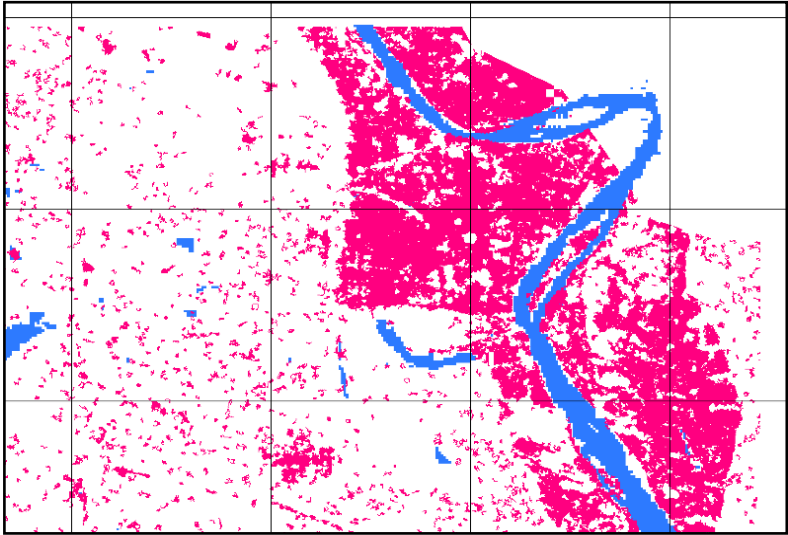


Fig 13: Random Forest

Classification Report:

	precision	recall	f1-score	support
No Flood	0.26	0.33	0.29	130
Flood	0.83	0.78	0.80	546
accuracy		0.69		676
macro avg	0.55	0.56	0.55	676
weighted avg	0.72	0.69	0.71	676

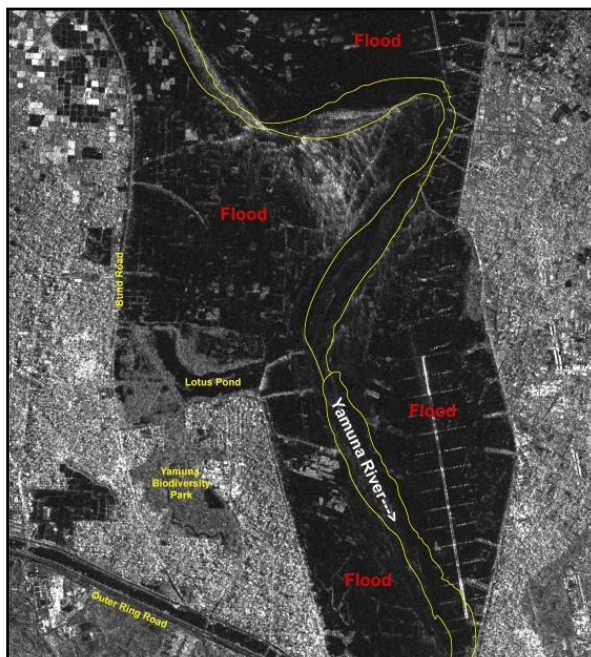


Fig 14: Reference Flood map from NRSC for Delhi

5.2 Chennai Results

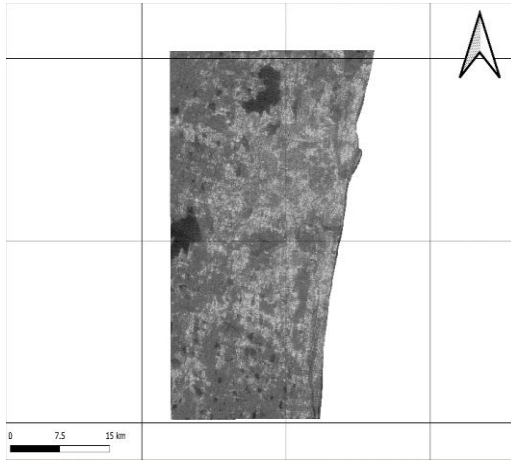


Fig 15: Before Flood

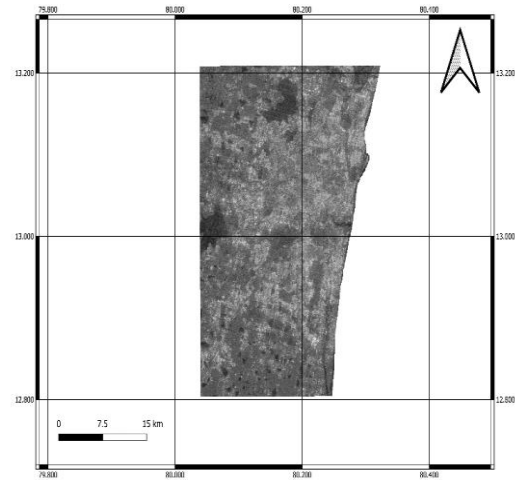


Fig 16: After Flood

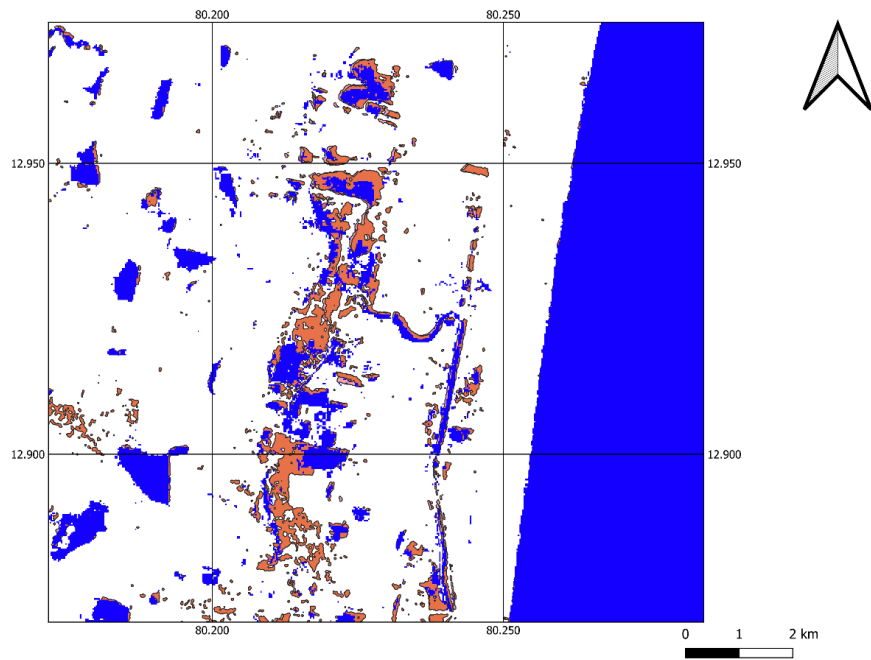


Fig 17: Rule based classification

precision	recall	f1-score	support	
0	0.55	0.26	0.36	99
1	0.74	0.91	0.81	225
accuracy		0.71	324	
macro avg	0.64	0.58	0.58	324
weighted avg	0.68	0.71	0.67	324

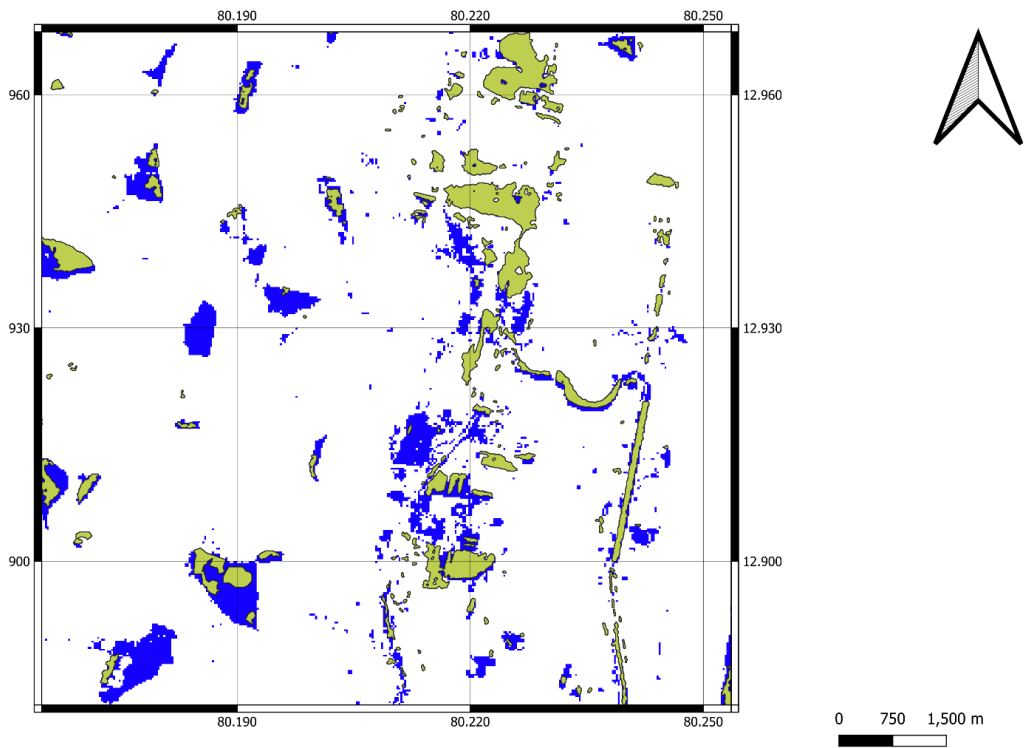


Fig 18: Change detection

	precision	recall	f1-score	support
0	0.30	0.22	0.26	99
1	0.69	0.77	0.73	225
accuracy			0.60	324
macro avg	0.50	0.50	0.49	324
weighted avg	0.57	0.60	0.59	324

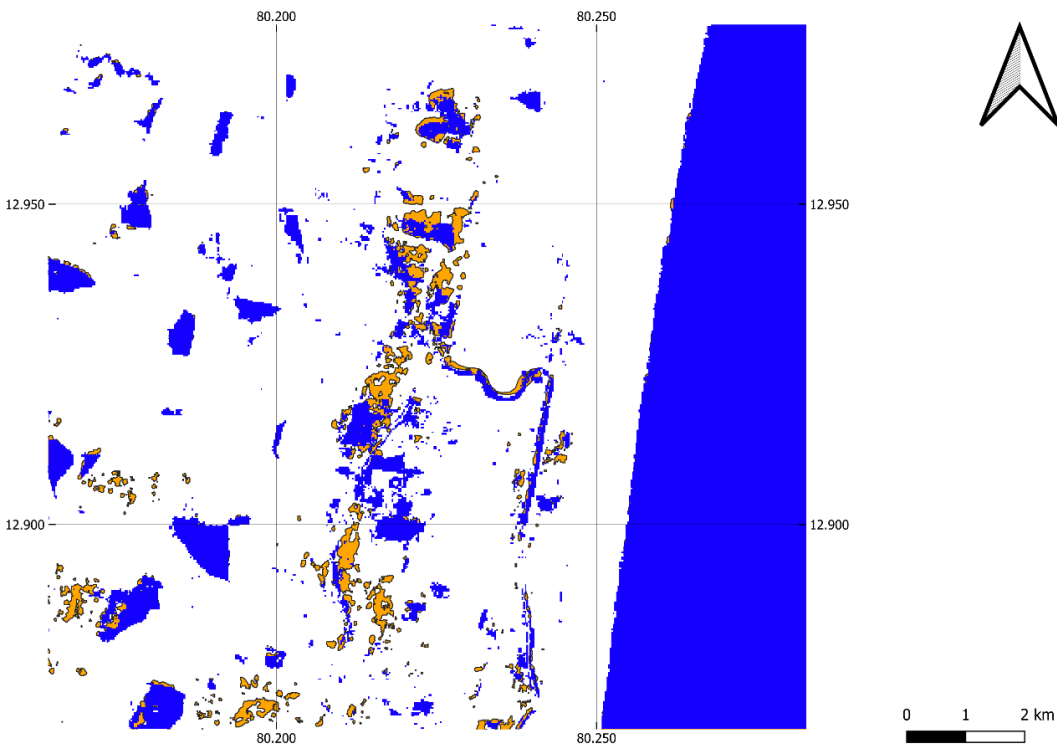


Fig 19: Random Forest

Classification Report:

	precision	recall	f1-score	support
0	0.00	0.00	0.00	99
1	0.69	1.00	0.82	225
accuracy			0.69	324
macro avg	0.35	0.50	0.41	324
weighted avg	0.48	0.69	0.57	324

Method	Precision	Recall	f1	Accuracy
Rule Based Classification	0.69	0.77	0.73	60
Change Detection	0.74	0.94	0.81	71
Random Forest	0.69	0.82	0.7	79

Fig 20: Comparison amongst methods for Chennai

5.3 Nagpur Results

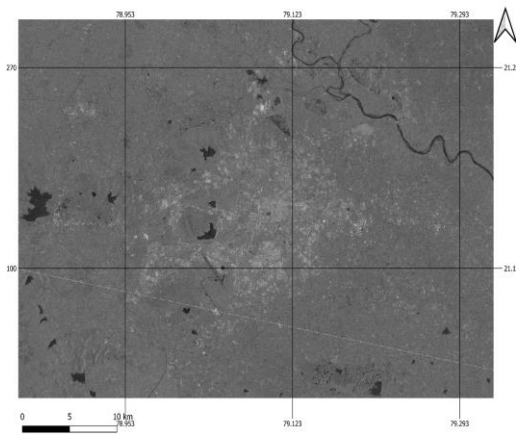


Fig 21: Before Flood

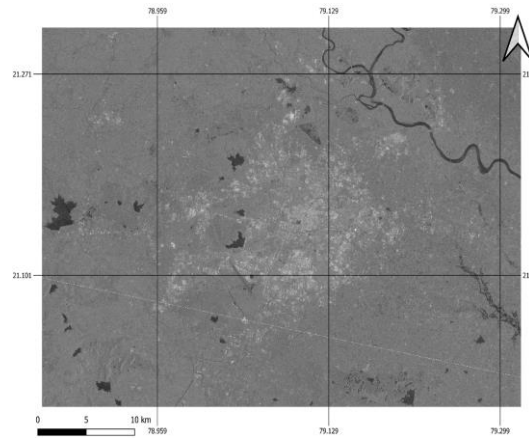


Fig 22: After Flood

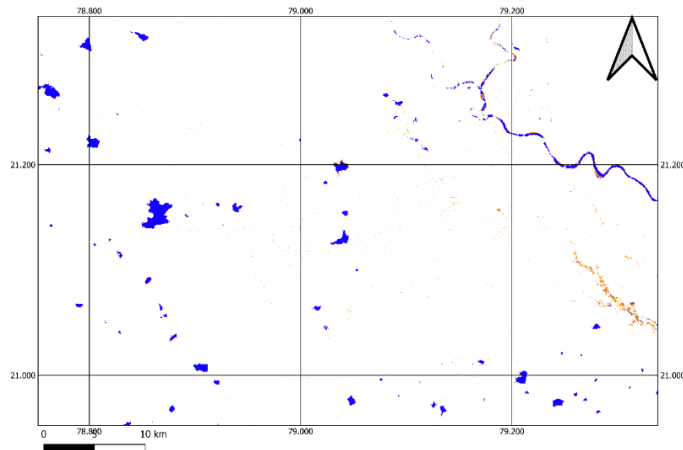
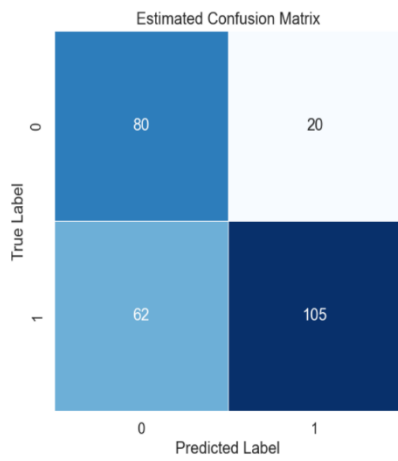


Fig 23: Rule based classification

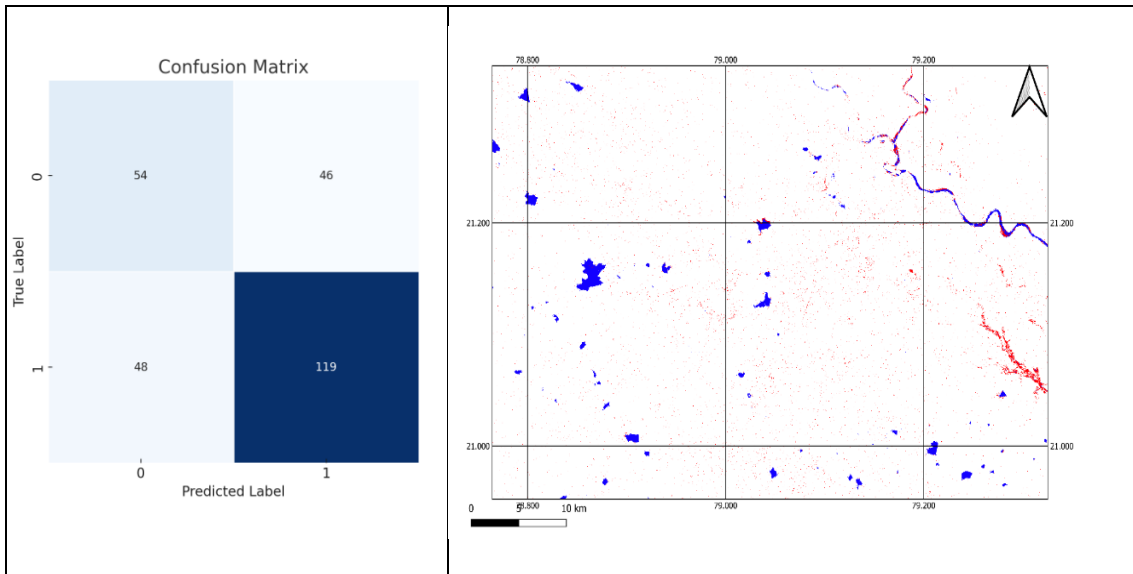


Fig 24: Change detection

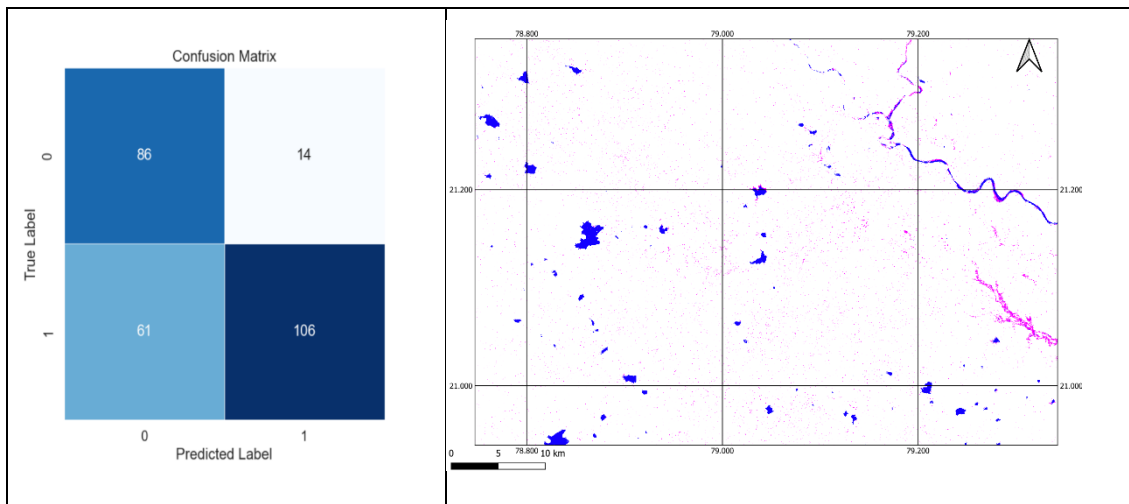


Fig 25: Random Forest

Method	Precision	Recall	f1	Accuracy	
Rule Based Classification	0.84	0.63	0.72	70	
Change Detection	0.73	0.71	0.72	66	
Random Forest	0.88	0.63	0.74	0.72	
weighted avg		0.66	0.66	0.66	267

Fig 26: Comparison amongst methods for Nagpur

5.4 Greece Results

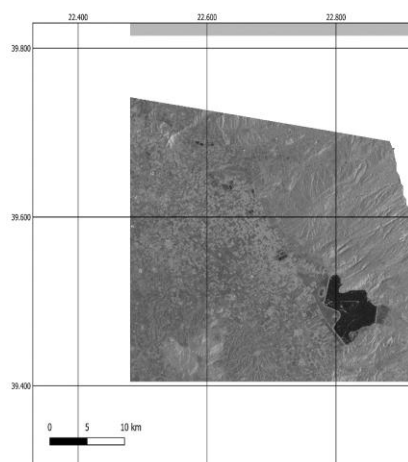


Fig 27: Before Flood

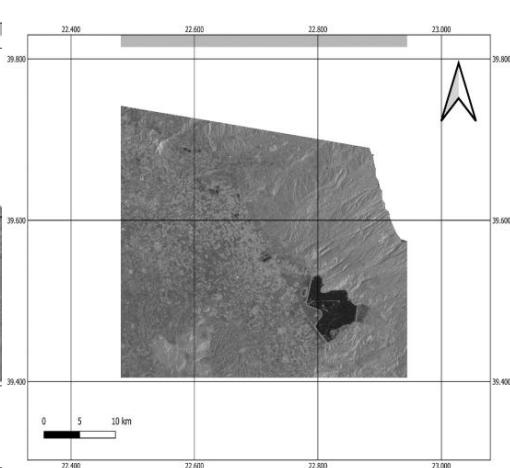


Fig 28: After Flood

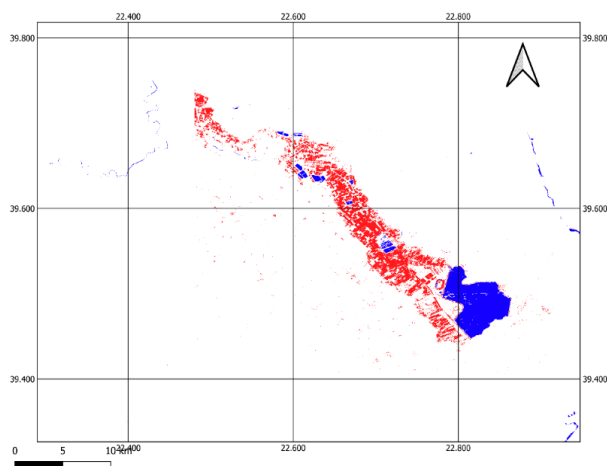
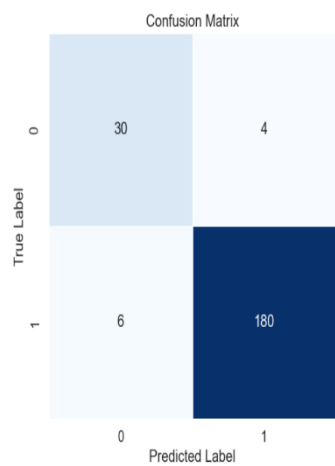


Fig 29: Rule based classification

Classification Report:

	precision	recall	f1-score	support
No Flood	0.26	0.47	0.34	30
Flood	0.90	0.79	0.85	190
accuracy			0.75	220
macro avg	0.58	0.63	0.59	220
weighted avg	0.82	0.75	0.78	220

Classification Report:

	precision	recall	f1-score	support
No Flood	0.26	0.73	0.38	30
Flood	0.94	0.67	0.78	190
accuracy			0.68	220
macro avg	0.60	0.70	0.58	220
weighted avg	0.85	0.68	0.73	220

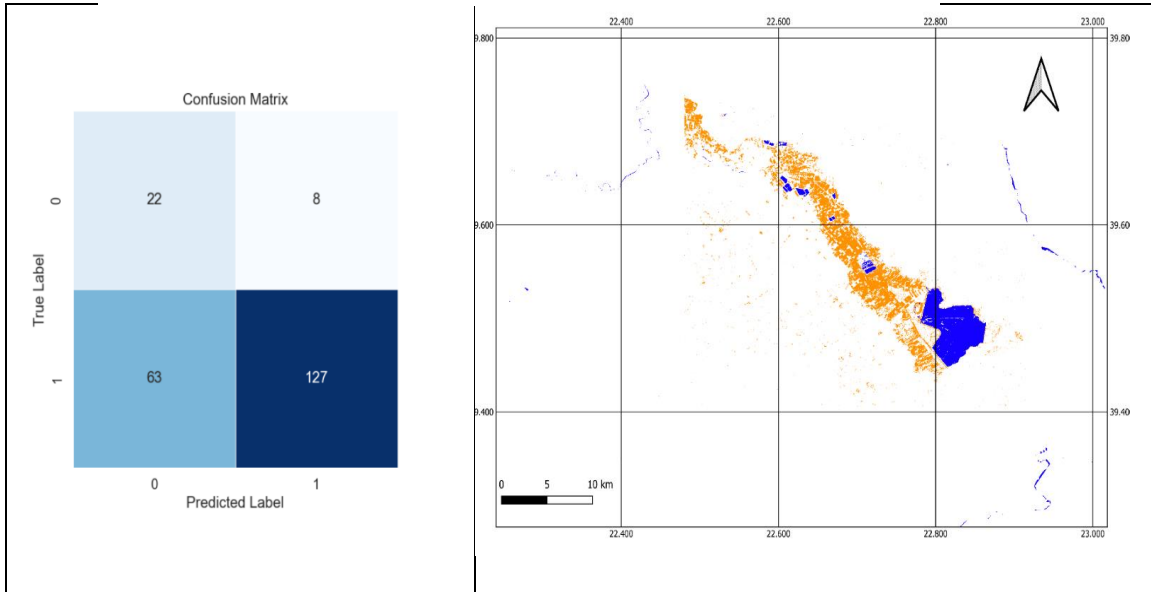


Fig 30: Change detection

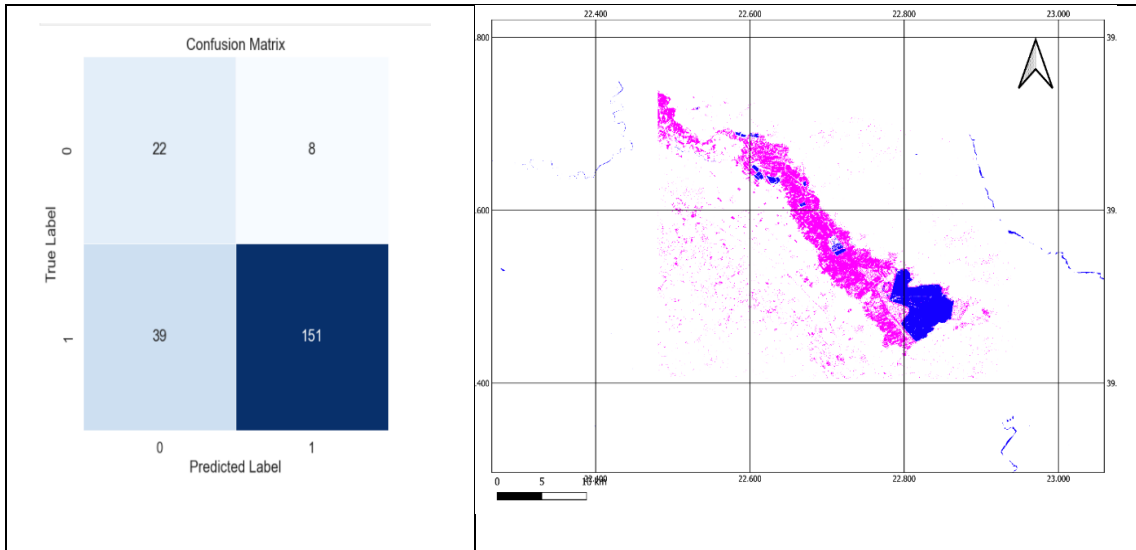


Fig 31: Random Forest

Classification Report:

	precision	recall	f1-score	support
No Flood	0.36	0.73	0.48	30
Flood	0.95	0.79	0.87	190
accuracy			0.79	220
macro avg	0.66	0.76	0.67	220
weighted avg	0.87	0.79	0.81	220

Method	Precision	Recall	f1	Accuracy
Rule Based Classification	0.9	0.7	0.85	75
Change Detection	0.94	0.67	0.78	68
Support Vector	0.85	0.76	0.87	67

Fig 32: Comparison amongst methods for Nagpur

--	--	--	--	--

Chapter 6

Conclusion

In the flood-affected regions of North Delhi, including areas like Signature Bridge, Old Delhi, Gandhi Vihar Wazirabad, Majnu Ka Tila, and Kashmere Gate, the Synthetic Aperture Radar (SAR) images captured during the flood event revealed a distinct pattern. The RGB composite of the images highlighted the presence of flooded areas, particularly noticeable in the eastern part of Delhi, encompassing regions like Geeta Colony, Shastri Park, and Mandawali. The most affected zones, including Khajuri Khas, Gokulpuri, and Sonia Vihar in Northeast Delhi, were also discernible.

What stands out in both the RGB and SAR images is the representation of flooded pixels in black. This characteristic black color is a result of the backscatter behavior in SAR data. SAR sensors emit microwave signals that interact with the Earth's surface, and the backscattered signals are recorded. In the case of flood mapping, water surfaces typically exhibit low radar backscatter, leading to darker tones in SAR imagery.

The dark pixels observed in both RGB and SAR images signify areas that experienced inundation during the flood event. The diminished radar backscatter from flooded regions contrasts with the higher backscatter from non-flooded surfaces like built-up areas or vegetation. This stark contrast in backscatter response serves as a visual cue, allowing for the identification and delineation of flooded areas in the imagery. Therefore, the black pixels in the images play a crucial role in visually indicating the extent of the flooded regions, aligning with the characteristic backscatter response of water surfaces in SAR imagery.

- More ground truth data will increase the accuracy of the model.
- For Urban Floods Random Forest performed better followed by Thresholding and Change detection.

In urban areas due to various complex urban backscatter patterns, including double bounce, shadow, and layover, which cause misclassification and increase false alarms

6.1 Future Work

In the future, a **robust validation** is planned to assess the accuracy and reliability of the flood mapping algorithm. This endeavor will involve a meticulous field validation process, during flood events in the current study area. By physically visiting the location, ground truth data, such as water levels and flood extent, will be gathered to validate the satellite-derived flood maps. This validation process will be complemented by a

detailed comparative analysis, incorporating quantitative metrics like accuracy, precision, recall, and F1 score.

A key focus is directed towards applying the developed flood mapping algorithm to a different Area of Interest (AOI). This strategic expansion aims to assess the algorithm's versatility and performance across diverse geographical settings, encompassing varying topography, hydrological conditions, and land use patterns. By deploying the algorithm in a distinct AOI, it becomes possible to evaluate its generalizability and uncover any region-specific nuances that may influence its effectiveness. Separate Paddy fields with the flooded pixels.

REFERENCES

1. Filipponi, F. Sentinel-1 GRD Preprocessing Workflow. *Proceedings* **2019**, *18*, 11. <https://doi.org/10.3390/ECRS-3-06201>
2. E. Hamidi, B. G. Peter, D. F. Muñoz, H. Mofstakhari and H. Moradkhani, "Fast Flood Extent Monitoring With SAR Change Detection Using Google Earth Engine," in *IEEE Transactions on Geoscience and Remote Sensing*, vol. 61, pp. 1-19, 2023, Art no. 4201419, doi: 10.1109/TGRS.2023.3240097.
3. Ali, M.A.S., 2007. September 2004 Flood Event in South western Bangladesh: A Study of its Nature, Causes and Human Perception and Adjustments to a New Hazard. *Natural Hazards*, 40: 89–111.
- 4 Benz, U.C., Hofmann, P., Willhauck, G., Lingenfelder, I. and Heynen, M., 2004. Multi resolution, object-oriented fuzzy analysis of remote sensing data for GIS-ready information. *ISPRS Journal of Photogrammetry & Remote Sensing*, 58: 239-258.
5. Chittibabu, P., 2004. Mitigation of Flooding and Cyclone Hazard in Orissa, India. *Natural Hazards*, 31: 455–485.
6. Huang, X. et al., 2008. Flood hazard in Hunan province of China: an economic loss analysis. *Natural Hazards*, 47: 65–73.
7. H. R. Pourghasemi et al., "Assessment of Urban Infrastructures Exposed to Flood Using Susceptibility Map and Google Earth Engine," in *IEEE Journal of Selected Topics in Applied Earth Observations and Remote Sensing*, vol. 14, pp. 1923-1937, 2021, doi: 10.1109/JSTARS.2020.3045278.
8. Armenakis, C.; Du, E.X.; Natesan, S.; Persad, R.A.; Zhang, Y. Flood Risk Assessment in Urban Areas Based on Spatial Analytics and Social Factors. *Geosciences* 2017, 7, 123. <https://doi.org/10.3390/geosciences7040123>
9. A. M. Al-Abadi, S. Shahid and A. K. Al-Ali, "A GIS-based integration of catastrophe theory and analytical hierarchy process for mapping flood susceptibility: A case study of Teeb area Southern Iraq", *Environ. Earth Sci.*, vol. 75, no. 8, 2016.
10. S. F. Sherpa and M. Shirzaei, "Country-wide flood exposure analysis using Sentinel-1 synthetic aperture radar data: Case study of 2019 Iran flood", *J. Flood Risk Manag.*, vol. 15, no. 1, pp. e12770, Mar. 2022.
11. A. AghaKouchak et al., "Climate extremes and compound hazards in a warming world", *Annu. Rev. Earth Planet. Sci.*, vol. 48, no. 1, pp. 519-548, May 2020.

12. V. S. K. Vanama, Y. S. Rao and C. M. Bhatt, "Change detection based flood mapping using multitemporal Earth observation satellite images: 2018 flood event of Kerala India", *Eur. J. Remote Sens.*, vol. 54, no. 1, pp. 42-58, Jan. 2021

13. Imran, M., Castillo, C., Lucas, J., Meier, P., & Vieweg, S. (2014). AIDR: Artificial Intelligence for Disaster Response. Proceedings of the 23rd International Conference on World Wide Web, 159-162.

14. Smith, L. C., & Ashmore, P. (2020). Online social media for integrated flood data analytics. *Nature Communications*, 11(1), 1-3.

15. Yin, J., & Wang, J. (2016). Social media data mining for urban flood mapping: A review. *International Journal of Disaster Risk Reduction*, 19, 237-244.

16. Gonzalez, R. C., & Woods, R. E. (2002). *Digital Image Processing*. Prentice Hall.

17. Otsu, N. (1979). A threshold selection method from gray-level histograms. *IEEE Transactions on Systems, Man, and Cybernetics*, 9(1), 62-66.

18. Zhang, H., & Xiao, Z. (2015). Flood detection and mapping using SAR data. *International Journal of Remote Sensing*, 36(23), 5962-5976.

19. National Remote Sensing Centre (NRSC), ISRO. (2021). *Flood Mapping Services*. NRSC Flood Services

20. OpenStreetMap. (2021). *OpenStreetMap Data*. OpenStreetMap

21. Copernicus Emergency Management Service (CEMS). (2021). *Rapid Mapping Products*. Copernicus EMS

22. Breiman, L. (2001). Random forests. *Machine Learning*, 45(1), 5-32.

23. H. R. Pourghasemi et al., "Assessment of Urban Infrastructures Exposed to Flood Using Susceptibility Map and Google Earth Engine," in *IEEE Journal of Selected Topics in Applied Earth Observations and Remote Sensing*, vol. 14, pp. 1923-1937, 2021, doi: 10.1109/JSTARS.2020.3045278.

24. Armenakis, C.; Du, E.X.; Natesan, S.; Persad, R.A.; Zhang, Y. Flood Risk Assessment in Urban Areas Based on Spatial Analytics and Social Factors. *Geosciences* 2017, 7, 123. <https://doi.org/10.3390/geosciences7040123>

25. A. M. Al-Abadi, S. Shahid and A. K. Al-Ali, "A GIS-based integration of catastrophe theory and analytical hierarchy process for mapping flood susceptibility: A case study of Teeb area Southern Iraq", *Environ. Earth Sci.*, vol. 75, no. 8, 2016

26. S. F. Sherpa and M. Shirzaei, "Country-wide flood exposure analysis using Sentinel-1 synthetic aperture radar data: Case study of 2019 Iran flood", *J. Flood Risk Manag.*, vol. 15, no. 1, pp. e12770, Mar. 2022.

27. A. AghaKouchak et al., "Climate extremes and compound hazards in a warming world", *Annu. Rev. Earth Planet. Sci.*, vol. 48, no. 1, pp. 519-548, May 2020.

28. V. S. K. Vanama, Y. S. Rao and C. M. Bhatt, "Change detection based flood mapping using multitemporal Earth observation satellite images: 2018 flood event of Kerala India", *Eur. J. Remote Sens.*, vol. 54, no. 1, pp. 42-58, Jan. 2021